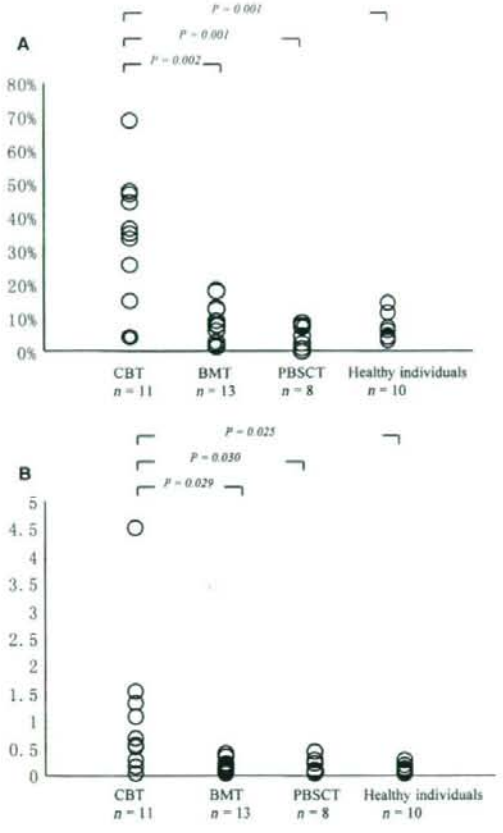

Figure 2 The proportion (A) and the absolute count (B) of $CD3^-CD16^+CD56^-$ in the PB of SCT recipients and healthy individuals. An increase in the proportion of $CD3^-CD16^+CD56^-$ NK cells (20% or more) in the PB $CD16^+$ NK cells and an increase in the absolute count of the same NK cell subset ($>0.5 \times 10^9$/L) were observed in seven of 11 CBT recipients, but in none of allogeneic 13 BM and eight PBSC transplant recipients. The $CD3^-CD16^+CD56^-$ cell count was calculated by multiplying the WBC count with the proportion (%) of this subset among the total cell event.

(Table 1). All $CD16^+CD56^-$ cells, similarly to $CD16^+CD56^+$ cells, expressed CD11a, CD18, but did not express a B-cell marker CD19, or the myeloid marker CD33 (data not shown). There were no differences in the expression levels of two major inhibitory NK receptors CD158a and CD158b between the two NK cell subsets (data not shown). On the other hand, the proportions of cells expressing activating NK receptors including NKG2D in $CD16^+CD56^-$ NK cells tended to be lower than those of $CD16^+CD56^+$ NK cells.

The leukemic cells obtained from Patient 1 before CBT exhibited an NKG2D ligand ULBP2 (Fig. 3). When the leukemic cells obtained after relapse was examined, the ULBP2 expression was observed to have decreased to levels comparable to ULBP1 and ULBP3.

Phenotypic change of $CD16^+CD56^-$ NK cells after *in vitro* culture

$CD16^+CD56^-$ NK cells derived from CB are reported to undergo differentiation *in vitro* in the presence of IL-2 (15, 21) and are therefore thought to be precursors of $CD16^+CD56^+$ NK cells (15). $CD16^+CD56^-$ NK cells were enriched from PBMCs of Patient 1 and Patient 2 and cultured in the presence of 100 IU/ml of IL-2 with or without irradiated K562-mb15-41BBL. In accordance with the results of previous studies, $CD16^+CD56^-$ NK cells from Patient 1 became $CD16^+CD56^+$ after *in vitro* culture (Fig. 4). Cultured $CD16^+CD56^-$ NK showed a tendency toward an increased expression of activating receptors including NKp30, NKp44, NKp46 and NKG2D, but did not show any changes in the expression of inhibitory receptors including CD158a, CD158b and NKG2A (Table 1).

Specificity of cultured $CD16^+CD56^-$ NK cells

Although attaining molecular remission in association with an increase in the $CD16^+CD56^-$ NK cells suggests the involvement of these NK cells in the GVL effect,

Table 1 Phenotype of the NK cell subsets from two CBT recipients

			NKp30		NKp44		NKp46		NKG2D	
			%	MFI	%	MFI	%	MFI	%	MFI
Patient 1	$CD56^+CD16^+$	Fresh	3.7	11.5	0	7.51	56.7	37.9	61.0	35.6
		Cultured	43.1	33.2	71.2	88.9	61.3	48.1	100.0	156.0
	$CD56^+CD16^-$	Fresh	0.0	8.37	0.0	7.57	17.6	12.6	46.7	12.6
		Cultured	14.2	10.4	51.4	31.0	54.2	26.8	99.9	26.8
Patient 2	$CD56^+CD16^+$	Fresh	3.6	6.71	0.0	7.72	42.9	44.3	72.3	44.3
		Cultured	14.2	39.4	51.4	49.4	54.2	54.4	99.5	54.4
	$CD56^+CD16^-$	Fresh	0.0	8.65	0.0	8.31	21.5	16.9	69.0	16.9
		Cultured	58.1	47.6	66.3	51.4	75.2	64.8	98.5	64.8

$CD16^+CD56^-$ and $CD16^+CD56^-$ NK cells were isolated from two CBT recipients and cultured with irradiated K562-mb15-41BBL in the presence of IL-2 for 14 d. Cultured NK showed increased expression of activating NK receptors including NKp30, NKp44, NKp46 and NKG2D.

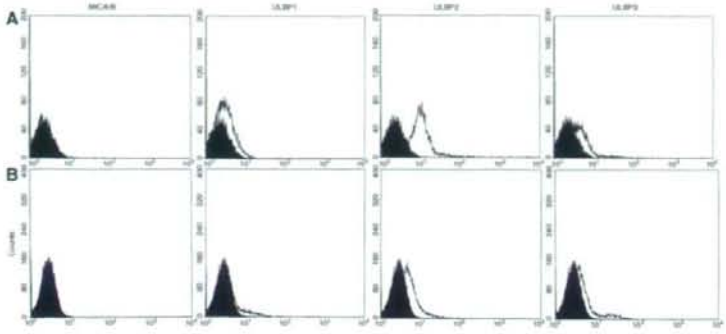

Figure 3 Expression of NKG2D ligands on leukemic cells from Patient 1. (A) leukemic cells obtained before CBT; (B) leukemic cells obtained after relapse. The proportion of ULBP2 expressing leukemic cells decreased from 59% to 9%.

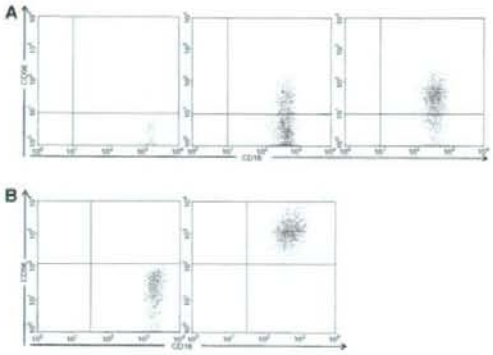

Figure 4 Phenotypic change of CD16⁺CD56⁻ NK cells with time associated with *in vitro* culture. Isolated CD16⁺CD56⁻ cells from Patient 1 were cultured in the presence of 100 IU/L IL-2 without (A) or with K562-mb15-41BBL (B). CD16⁺CD56⁻ NK cells from CBT recipients became CD16⁺CD56⁺ after the *in vitro* culture.

there was no killer-cell immunoglobulin receptor (KIR)-ligand (KIR-L) mismatch between Patient 1 and the CB donor; Patient 1 and the CB donor shared C*0102 and C*0304. To determine whether cultured NK cells derived from CD16⁺CD56⁻ NK cells retain specificity restricted by KIR-L of target cells, cultured NK cells from Patient 1 and Patient 2 who possessed C*0102 and C*1202 were separated into CD158b⁺ and CD158b⁻ NK cells, and were examined for their cytotoxicity against 721–221 cells transfected with different HLA-C alleles (Fig. 5). CD158b⁺ NK cells failed to kill 721–221 cells transfected with HLA-C*0301 (.221-Cw3) while they killed both wild-type 721–221 cells and 721–221 cells transfected with HLA-C*0401 (.221-Cw4). Conversely, CD158b⁻ NK cells not only killed 721–221 cells but they also killed .221-Cw3 and .221-Cw4 cells, thus indicating that the cytotoxicity due to the cultured CD158b⁺ NK cells is inhibited by the KIR-L Cw3 of the target cells.

Cytotoxicity of cultured CD16⁺CD56⁻ NK cells against leukemic cells

When leukemic cells obtained from Patient 1 before CBT were used as a target, both CD158b⁺ and CD158b⁻ NK cells showed similar cytotoxicity to that of unfractionated NK cells (Fig. 6). The cytotoxicity was blocked by

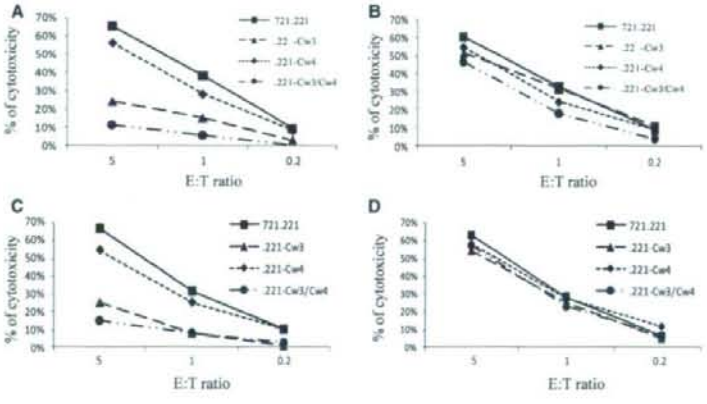

Figure 5 Specificity of NK cells derived from CD16⁺CD56⁻ NK cells. Cultured NK cells derived from CD16⁺CD56⁻ cells of Patient 1 (A and B) and Patient 2 (C and D) were separated into CD158b⁺ (A and C) and CD158b⁻ cells (B and D) and were examined for the cytotoxicity against 721-221 cells and 721-221 transfected with different HLA-C alleles C*0301 (.221-Cw3) and C*0401 (.221-Cw4). The data represent one of two experiments which produced similar results.

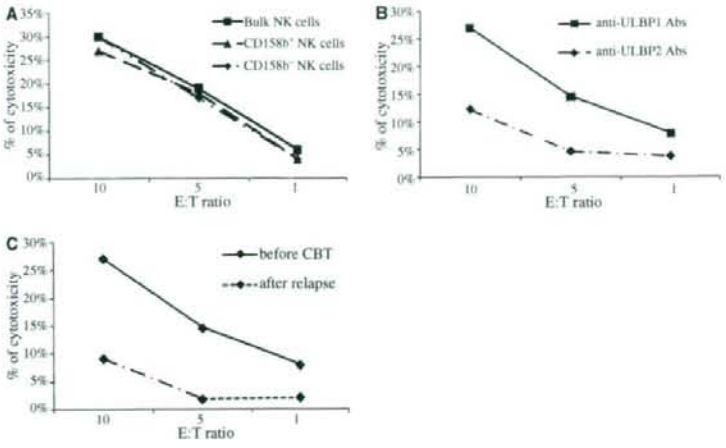

Figure 6 Cytotoxicity of cultured NK cells against leukemic cells. (A) Unseparated and separated NK cells were tested against leukemic cells obtained before CBT; (B) Leukemic cells were incubated in the presence of anti-ULBP1 or ULBP2 Abs before incubation with cultured NK cells; (C) Cytotoxicity of unseparated NK cells were tested against leukemic cells obtained before CBT or after relapse. The data represent one of three experiments which produced similar results.

treatment of leukemia cells with anti-ULPB2 mAbs. Leukemic cells obtained after relapse were relatively resistant to killing by cultured NK cells in comparison to those obtained before CBT.

Discussion

The present study revealed an increase in a unique NK cell subset characterized by CD16$^+$CD56$^-$ in CBT recipients. Although CD3$^-$CD16$^+$CD56$^-$ cells comprise monocytes, an increase in this subset was due to an increase in immature NK cells because they did not express a myeloid marker CD33 and acquired CD56 expression by *in vitro* culture in the presence of IL-2. An increase in NK cells with a similar phenotype has been shown in patients with solid tumors who were treated with IL-2 (21) and in those with HIV infection (22). Our CBT recipients did not receive cytokine therapy nor show any signs of viral infections at sampling. The expression of KIRs including CD158a and CD158b was not depressed in CD16$^+$CD56$^-$ cells of Patient 1 and Patient 2 in contrast to those of HIV patients (22). An *in vitro* culture of CD16$^+$CD56$^-$ NK cells from patients with HIV viremia in the presence IL-2 reportedly failed to induce NKp44 expression while it did induce the NKp44 expression by CD16$^+$CD56$^-$ NK cells from the two CBT recipients. It is therefore unlikely that the increase in the CD16$^+$CD56$^-$ cell count in the CBT recipients was secondary to viral infections.

Gaddy *et al.* demonstrated a novel subset of NK cells characterized by a phenotype CD16$^+$CD56$^-$ to exist in CB (12). They hypothesized that this NK cell subset represents immature NK cells capable of differentiating into CD16$^+$CD56$^+$ NK cells (15). CD16$^+$CD56$^-$ cells of our patients also underwent differentiation into CD16$^+$CD56$^+$ cells when they were cultured in the presence of IL-2. Therefore, CD16$^+$CD56$^-$ cells in PB after CBT may be derived from immature NK cells or NK precursor cells which existed in CB grafts. Previous studies on NK cells from SCT recipients and *ex vivo* engineered CB NK cells did not reveal an increased proportion of CD16$^+$CD56$^-$ cells (23–25). Both Patient 1 and Patient 2 received an HLA-mismatched CB graft although there was no KIR-L mismatch. Notably, Patient 1 had a large leukemic burden at the time of reduced-intensity preconditioning. It is therefore plausible that residual leukemic cells may have stimulated NK cell precursors to recruit CD16$^+$CD56$^-$ NK cells in Patient 1.

Patient 1's leukemic cells obtained before CBT expressed ULBP2. The incubation of CD16$^+$CD56$^-$ NK cells derived from Patient 1 in the presence of IL-2 and the K562 transfectant augmented NKG2D expression and the cultured NK cells showed cytotoxicity against leukemic cells despite that cultured NK cells retained KIR-L specificity and Patient 1's leukemic cells expressed matched KIR-L HLA-C*0304/C*0102. The cytotoxicity by the cultured NK cells decreased against leukemic cells treated with anti-ULBP2 Abs, and also against the leukemic cells obtained from Patient 1 after relapse which were devoid of ULBP2 expression. These findings suggest that mature NK cells derived from CD16$^+$CD56$^-$ NK cells may have exerted GVL effect on Patient 1's leukemic cells by way of interaction of NKG2D and ULBP2. The aberrant expression of NKG2D ligands by leukemic cells has been demonstrated by previous studies (26), but its influence on the outcome of allogeneic SCT has not yet been clarified. The results of the present study

indicate that the susceptibility of leukemic cells to NK cells may depend on both expression of NKG2D ligand on leukemic cells and the expression of NKG2D on effector NK cells. In patients with acute leukemia, leukemic cells are reported to downregulate NKp30 of autologous NK cells, thereby allowing NK cells to escape leukemic cells (27, 28). In the setting of CBT, leukemic cells expressing NKG2D ligands may tend to stimulate NK cell precursors in CB, thus inducing them to undergo differentiation.

The present study demonstrated the expansion of CD16$^+$CD56$^-$ NK cells in the PB of CBT recipients for the first time. These immature NK cells can be expanded *ex vivo* with a help of K562-mb15-41BBL cells as maintaining specificity to KIR-L and cytotoxicity against leukemic cells expressing an NKG2D ligand. Therefore, CB may be a potential source of NK cells which can be utilized for cell therapy. Further studies on a larger number of CBT recipients are needed to determine whether CD16$^+$CD56$^-$ NK cells indeed play a role in the GVL effect.

Acknowledgement

We thank Dr. Dario Campana and Dr Chihaya Imai for providing us with K562-mb15-41BBL cells.

References

1. Takahashi S, Ooi J, Tomonari A, *et al.* Comparative single-institute analysis of cord blood transplantation from unrelated donors with bone marrow or peripheral blood stem-cell transplants from related donors in adult patients with hematologic malignancies after myeloablative conditioning regimen. *Blood* 2007;**109**:1322–30.
2. Arcese W, Rocha V, Labopin M, *et al.* Unrelated cord blood transplants in adults with hematologic malignancies. *Haematologica* 2006;**91**:223–30.
3. Rocha V, Cornish J, Sievers EL, *et al.* Comparison of outcomes of unrelated bone marrow and umbilical cord blood transplants in children with acute leukemia. *Blood* 2001;**97**:2962–71.
4. Barker JN, Weisdorf DJ, DeFor TE, Blazar BR, McGlave PB, Miller JS, Verfaillie CM, Wagner JE. Transplantation of 2 partially HLA-matched umbilical cord blood units to enhance engraftment in adults with hematologic malignancy. *Blood* 2005;**105**:1343–7.
5. Harris DT, Schumacher MJ, Locascio J, Besencon FJ, Olson GB, DeLuca D, Shenker L, Bard J, Boyse EA. Phenotypic and functional immaturity of human umbilical cord blood T lymphocytes. *Proc Natl Acad Sci U S A* 1992;**89**:10006–10.
6. Ruggeri L, Capanni M, Casucci M, Volpi I, Tosti A, Perruccio K, Urbani E, Negrin RS, Martelli MF, Velardi A. Role of natural killer cell alloreactivity in HLA-mismatched hematopoietic stem cell transplantation. *Blood* 1999;**94**:333–9.
7. Ruggeri L, Capanni M, Urbani E, *et al.* Effectiveness of donor natural killer cell alloreactivity in mismatched hematopoietic transplants. *Science* 2002;**295**:2097–100.
8. Cooley S, McCullar V, Wangen R, Bergemann TL, Spellman S, Weisdorf DJ, Miller JS. KIR reconstitution is altered by T cells in the graft and correlates with clinical outcomes after unrelated donor transplantation. *Blood* 2005;**106**:4370–6.
9. Komanduri KV, St John LS, de Lima M, *et al.* Delayed immune reconstitution after cord blood transplantation is characterized by impaired thymopoiesis and late memory T cell skewing. *Blood* 2007;**110**:4543–51.
10. Giraud P, Thuret I, Reviron D, Chambost H, Brunet C, Novakovitch G, Farnarier C, Michel G. Immune reconstitution and outcome after unrelated cord blood transplantation: a single paediatric institution experience. *Bone Marrow Transplant* 2000;**25**:53–7.
11. Locatelli F, Maccario R, Comoli P, *et al.* Hematopoietic and immune recovery after transplantation of cord blood progenitor cells in children. *Bone Marrow Transplant* 1996;**18**:1095–101.
12. Gaddy J, Risdon G, Broxmeyer HE. Cord blood natural killer cells are functionally and phenotypically immature but readily respond to interleukin-2 and interleukin-12. *J Interferon Cytokine Res* 1995;**15**:527–36.
13. Bradstock KF, Luxford C, Grimsley PG. Functional and phenotypic assessment of neonatal human leucocytes expressing natural killer cell-associated antigens. *Immunol Cell Biol* 1993;**71**:535–42.
14. Phillips JH, Hori T, Nagler A, Bhat N, Spits H, Lanier LL. Ontogeny of human natural killer (NK) cells: fetal NK cells mediate cytolytic function and express cytoplasmic CD3 epsilon,delta proteins. *J Exp Med* 1992;**175**:1055–66.
15. Gaddy J, Broxmeyer HE. Cord blood CD16$^+$56$^-$ cells with low lytic activity are possible precursors of mature natural killer cells. *Cell Immunol* 1997;**180**:132–42.
16. Igarashi T, Wynberg J, Srinivasan R, Becknell B, McCoy JP Jr, Takahashi Y, Suffredini DA, Linehan WM, Caligiuri MA, Childs RW. Enhanced cytotoxicity of allogeneic NK cells with killer immunoglobulin-like receptor ligand incompatibility against melanoma and renal cell carcinoma cells. *Blood* 2004;**104**:170–7.
17. Imai C, Iwamoto S, Campana D. Genetic modification of primary natural killer cells overcomes inhibitory signals and induces specific killing of leukemic cells. *Blood* 2005;**106**:376–83.
18. Kondo E, Topp MS, Kiem HP, Obata Y, Morishima Y, Kuzushima K, Tanimoto M, Harada M, Takahashi T, Akatsuka Y. Efficient generation of antigen-specific cytotoxic T cells using retrovirally transduced CD40-activated B cells. *J Immunol* 2002;**169**:2164–71.
19. Nakao S, Takami A, Takamatsu H, *et al.* Isolation of a T-cell clone showing HLA-DRB1*0405-restricted

cytotoxicity for hematopoietic cells in a patient with aplastic anemia. *Blood* 1997;**89**:3691–9.
20. Ogawa H, Tamaki H, Ikegame K, *et al.* The usefulness of monitoring WT1 gene transcripts for the prediction and management of relapse following allogeneic stem cell transplantation in acute type leukemia. *Blood* 2003;**101**:1698–704.
21. McKenzie RS, Simms PE, Helfrich BA, Fisher RI, Ellis TM. Identification of a novel CD56$^-$ lymphokine-activated killer cell precursor in cancer patients receiving recombinant interleukin 2. *Cancer Res* 1992;**52**:6318–22.
22. Mavilio D, Lombardo G, Benjamin J, *et al.* Characterization of CD56$^-$/CD16$^+$ natural killer (NK) cells: a highly dysfunctional NK subset expanded in HIV-infected viremic individuals. *Proc Natl Acad Sci U S A* 2005;**102**:2886–91.
23. Jacobs R, Stoll M, Stratmann G, Leo R, Link H, Schmidt RE. CD16$^-$ CD56$^+$ natural killer cells after bone marrow transplantation. *Blood* 1992;**79**:3239–44.
24. Ayello J, van de Ven C, Fortino W, *et al.* Characterization of cord blood natural killer and lymphokine activated killer lymphocytes following ex vivo cellular engineering. *Biol Blood Marrow Transplant* 2006;**12**:608–22.
25. Moretta A, Maccario R, Fagioli F, *et al.* Analysis of immune reconstitution in children undergoing cord blood transplantation. *Exp Hematol* 2001;**29**:371–9.
26. Salih HR, Antropius H, Gieseke F, Lutz SZ, Kanz L, Rammensee HG, Steinle A. Functional expression and release of ligands for the activating immunoreceptor NKG2D in leukemia. *Blood* 2003;**102**:1389–96.
27. Costello RT, Sivori S, Marcenaro E, Lafage-Pochitaloff M, Mozziconacci MJ, Reviron D, Gastaut JA, Pende D, Olive D, Moretta A. Defective expression and function of natural killer cell-triggering receptors in patients with acute myeloid leukemia. *Blood* 2002;**99**:3661–7.
28. Fauriat C, Just-Landi S, Mallet F, Arnoulet C, Sainty D, Olive D, Costello RT. Deficient expression of NCR in NK cells from acute myeloid leukemia: evolution during leukemia treatment and impact of leukemia cells in NCRdull phenotype induction. *Blood* 2007;**109**:323–30.

Int. J. Cancer: **122**, 2542–2553 (2008)

The DNA demethylating agent 5-aza-2′-deoxycytidine activates NY-ESO-1 antigenicity in orthotopic human glioma

Atsushi Natsume[1]*, Toshihiko Wakabayashi[1,2], Kunio Tsujimura[3]*, Shinji Shimato[1], Motokazu Ito[1], Kiyotaka Kuzushima[3], Yutaka Kondo[4], Yoshitaka Sekido[4], Hitomi Kawatsura[1], Yuji Narita[5] and Jun Yoshida[1,2]

[1]*Department of Neurosurgery, Nagoya University School of Medicine, Nagoya, Japan*
[2]*Center for Genetic and Regenerative Medicine, Nagoya University Hospital, Nagoya, Japan*
[3]*Division of Immunology, Aichi Cancer Center Research Institute, Nagoya, Japan*
[4]*Division of Molecular Oncology, Aichi Cancer Center Research Institute, Nagoya, Japan*
[5]*Department of Tissue Engineering, Nagoya University School of Medicine, Nagoya, Japan*

Cancer/testis antigens (CTAs) are considered to be suitable targets for the immunotherapy of human malignancies. It has been demonstrated that in a variety of tumors, the expression of certain CTAs is activated *via* the demethylation of their promoter CpG islands. In our study, we have shown that while the composite expression of 13 CTAs in 30 human glioma specimens and newly established cell lines from the Japanese population was nearly imperceptible, the DNA-demethylating agent 5-aza-2′-deoxycytidine (5-aza-CdR) markedly reactivated CTA expression in glioma cells but not in normal human cells. We quantified the diminished methylation status of NY-ESO-1-one of the most immunogenic CTAs-following 5-aza-CdR treatment by using a novel Pyrosequencing™ technology and methylation-specific PCR. Microarray analysis revealed that 5-aza-CdR is capable of signaling the immune system, particularly, human leukocyte antigen (HLA) class I upregulation. ^{51}Cr-release cytotoxicity assays and cold target inhibition assays using NY-ESO-1-specific cytotoxic T lymphocyte (CTL) lines demonstrated the presentation of *de novo* NY-ESO-1 antigenic peptides on the cell surfaces. In an orthotopic xenograft model, the systemic administration of 5-aza-CdR resulted in a significant volume reduction of the transplanted tumors and prolonged the survival of the animals after the adoptive transfer of NY-ESO-1-specific CTLs. These results suggested that 5-aza-CdR induces the expression of epigenetically silenced CTAs in poorly immunogenic gliomas and thereby presents a new strategy for tumor immunotherapy targeting 5-aza-CdR-induced CTAs.

Key words: glioma; cancer-testis antigens; DNA methylation; immunotherapy; NY-ESO-1

Over the last decade, there has been major progress in the identification and characterization of human tumor antigens recognized by the host immune system. A subgroup of tumor antigens, commonly referred to as cancer/testis antigens (CTAs), are expressed only in the tissues of the testis, ovary and placenta under normal conditions, but are also expressed in various types of human tumors.[1,2] Since normal CTA-expressing tissues do not express major histocompatibility complex (MHC) class I molecules, CD8 T cells cannot recognize CTAs expressed on these tissues, suggesting that CTAs are the ideal targets for tumor immunotherapy. CTAs and genes were originally identified through a variety of methods. These include T-cell epitope labeling,[3] serological analysis of cDNA expression libraries (SEREX),[4,5] differential gene expression analysis[6] and bioinformatics methods.[7–9] In particular, NY-ESO-1 is the most immunogenic CTA discovered thus far, and it is considered to be a highly promising therapeutic target for immunotherapy.[10] To date, very little is known regarding the physiological function(s) of these antigens or the mode in which the expression of their gene families is regulated.

Epigenetic alterations, including hypermethylation of promoter CpG islands, histone deacetylation of tumor suppressor and tumor-related genes,[11–13] and global DNA hypomethylation,[14,15] have been recognized as important contributors to carcinogenesis in humans. Global DNA hypomethylation has been observed in various neoplasms and is considered to occur at the early stages of tumor development.[16–18] However, it has been shown that the expression of certain CTA genes is reactivated in cancerous cells; this could be due to a loss of epigenetic regulation as observed when methylated chromatin regions are demethylated or when deacetylated histones are acetylated.[19] Therefore, recent evidence shows that the deregulation of the DNA methylation apparatus that occurs during cancer development could provide new therapeutic targets for cancer treatment.

The DNA demethylating agent 5-aza-2′-deoxycytidine (5-aza-CdR, decitabine) is a cytosine analogue that is incorporated into DNA during replication. It covalently binds DNA methyltransferase and inhibits its activity, leading to genome-wide demethylation.[20–24] There have been several studies demonstrating the ability of 5-aza-CdR to activate the gene expression of CTAs *in vitro* and *in vivo*, which may be silenced by the hypermethylation of their promoters. This drug has been used in clinical studies for the treatment of chronic myelogenous leukaemia (CML), sickle cell anaemia and myelodysplastic syndrome (MDS).[20,25–27] Previous evidence has clearly defined the epigenetic regulatory role of DNA methylation in the constitutive expression of CTAs by cutaneous melanoma cells and renal cancer cells and has demonstrated that *in vitro* treatment with 5-aza-CdR upregulated their expression in neoplastic cells.[28,29]

Gliomas are the most common primary tumors of the central nervous system; they account for 30% of adult primary brain tumors. Brain tumors remain difficult to cure despite recent advances in surgical, radiotherapeutic and chemotherapeutic approaches. In particular, there is currently no optimal treatment for glioblastoma multiforme, the most common malignant brain tumor in adults, and patients typically survive for a period less than a year. The poor outcome partly relates to the inability in delivering chemotherapeutic agents through the blood–brain barrier (BBB) and the low effect of radiation on the tumor. Therefore, new and more effective strategies are urgently required. Of these, the establishment of immunotherapy specifically targeting malignant cells is expected to improve tumor prognosis. It has recently been demonstrated that malignant glioma cells express certain known tumor-associated antigens such as HER-2, gp100, MAGE-

This article contains supplementary material available via the Internet at http://www.interscience.wiley.com/jpages/0020-7136/suppmat.

Grant sponsor: Grant-in-Aid for Scientific Research (B) from the Ministry of Health, Labor, and Welfare; Grant number: 18390395; Grant sponsor: the Japan Society for the Promotion of Science, Tokyo; Grant sponsor: the Third Team Comprehensive Control Research for Cancer from the Ministry of Health, Labor, and Welfare, Japan; Grant number: 26.

Kunio Tsujimura's current address is: Department of Infectious Diseases, Hamamatsu University School of Medicine, 1-20-1 Handa-yama, Higashi-ku, Hamamatsu 431-3192, Japan.

***Correspondence to:** Department of Neurosurgery, Nagoya University School of Medicine, 65 Tsurumai-cho, Showa-ku, Nagoya 466-8550, Japan. E-mail: anatsume@med.nagoya-u.ac.jp or ktsujimu@hama-med.ac.jp

Received 5 July 2007; Accepted after revision 4 December 2007
DOI 10.1002/ijc.23407
Published online 31 January 2008 in Wiley InterScience (www.interscience.wiley.com).

1 and IL-13 receptor α2.[30–37] However, CTA profiling of glioma cells, in particular, in the Asian population remains unknown.

In our study, we analyzed the expression of 13 CTA genes (*MAGE-1*, *MAGE-3*, *MAGE-4*, *MAGE-6*, *MAGE-10*, *MAGE-3/6*, *LAGE-1*, *CT7*, *SCP-1*, *SSX-1*, *SSX-2*, *SSX-4* and *NY-ESO-1*) in 30 glioma tissues, 5 human glioma cell lines and 3 newly established cell lines from the Japanese population. Subsequently, the role of 5-aza-CdR in the regulation of the expression of various CTAs in glioma cells was analyzed. Finally, we demonstrated that NY-ESO-1, one of the most antigenic CTAs, is effectively induced in human glioma cells by 5-aza-CdR, and that these glioma cells forcibly expressing NY-ESO-1 show *in vitro* and *in vivo* sensitivity to NY-ESO-1-specific cytotoxic T lymphocytes (CTLs). Our present study provides the basis to establish novel immunotherapeutic approaches in glioma patients.

Material and methods

Cells

The human glioma cell lines U251 (human leukocyte antigen (HLA)-A2), SKMG1 (HLA-A24), AO2 (HLA-A3), U87MG (HLA-A2) and T98 (HLA-A2) were obtained from the Memorial Sloan-Kettering Cancer Institute (New York, NY) and maintained in Eagle's minimal essential medium (MEM) at 37°C in a humidified atmosphere of 5% CO_2 in air. A human osteosarcoma cell line, namely, SaOS-2 (NY-ESO-1+, HLA-A2), was kindly provided by Dr. Y. Nishida (Department of Orthopaedics, Nagoya University, Nagoya, Japan) and maintained in Dulbecco's modified Eagle's medium (DMEM; Nissui, Tokyo, Japan). A human myeloid leukaemia cell line K562 and the HLA-A*0201-transfected T2 cell line (T2.A2) were maintained in RPMI 1640 (Invitrogen, Carlsbad, CA). The medium was supplemented with 10% fetal bovine serum (FBS), 5 mM L-glutamine, 2 mM nonessential amino acids, and antibiotics (100 U/ml penicillin and 100 μg/ml streptomycin). Commercially available normal human astrocytes (NHA; Cambrex, Baltimore, MD) maintained in AGM medium with BulletKit supplement (Cambrex), human aortic smooth muscle cells (AoSMC; Cambrex), human adult fibroblasts (NHDF-ad; Cambrex) maintained in DMEM with 10% FBS, and human epidermal keratinocytes (NHEK, Kurabo, Osaka, Japan) maintained in Epilife medium (Cascade Biologics, Nottinghamshire, UK) supplemented with HuMedia-KG (Kurabo) were used as normal cells.

Reagents and peptides

A vial containing 5 mg lyophilized powder of 5-aza-CdR was obtained (Sigma-Aldrich, St. Louis, MO). The vial was reconstituted with 20 ml sterile water to obtain a 1 mM solution, and it was stocked at 4°C. The HLA-A2-binding NY-ESO-1 peptide, p157-165 (SLLMWITQC), which was initially identified using the T-cell line NW38-1VS-1[38] and the HLA-A2-binding IL-13Rα2 peptide, p345-354 (WLPFGFILI), which was identified previously,[37] was synthesized by Thermo Electron GmbH (>90% purity) (Ulm, Germany), and solubilized in 50% dimethyl sulphoxide (DMSO)/water.

Collection of surgical specimens

Thirty tumor samples were collected at the Nagoya University School of Medicine from patients whose tumors were histologically diagnosed as gliomas (WHO Grade II, III and IV). Genetic analysis in our study was approved by the ethical committee of Nagoya University Hospital. All patients provided written informed consent. All tissues were frozen immediately and stored at −80°C until use.

Primary-culture cells derived from patients with high-grade gliomas

Tumor tissues were derived from 3 patients with high-grade gliomas who had undergone surgical resection in Nagoya University Hospital, Nagoya, Japan; the tissues were primary-cultured as follows. Immediately after the brain tumors were removed from the patients, the tissues were homogenized and digested with 1% DNase and 0.1% trypsin for 30 min at 37°C and centrifuged at 800 rpm for 5 min. The cells were seeded at a density of 2×10^6 cells per 100-mm dish and maintained in DMEM supplemented with 10% FBS, 5 mM L-glutamine, 2 mM nonessential amino acids, and antibiotics (100 U/ml penicillin and 100 μg/ml streptomycin). The cells were then incubated in a standard tissue culture incubator (100% relative humidity and 5% CO_2). After achieving 80–90% confluence, they were subcultured onto a new 100-mm plate at a density of 2×10^6. The established cell lines were designated as NNS-10, NNS-11 and NNS-12. All cells were immunocytochemically confirmed as glioma cells based on their expression of glial-fibrilliary acidic protein (GFAP).

In vitro *treatment of cultured cells with 5-aza-CdR*

Treatment with 5-aza-CdR was performed as described in a previous study.[29] Cells were seeded at a density of 1.0×10^5 cells/well in a 6-well plate, and placed at 37°C overnight in a 5% CO_2 incubator. The next day, the cell culture medium was replaced with fresh medium containing 0.1, 1 and 10 μM 5-aza-CdR. The medium was changed every 12 hr for 2 days. The plates were wrapped in aluminum foil to avoid light exposure. At the end of the treatment, the medium was replaced with fresh medium without 5-aza-CdR, and the cells were cultured for an additional 48 hr.

RNA extraction

RNA was isolated from 25 to 50 mg of tissue/sample by using Trizol (Invitrogen) according to the manufacturer's protocol. RNA was finally resuspended in nuclease-free water.

Conventional reverse transcription PCR

cDNA was synthesized from 1 μg total RNA by using random hexamers and the Superscript II reverse transcription (RT) kit (Invitrogen), according to the manufacturer's protocol. For each PCR, 2 μl cDNA was used in a 20-μl reaction volume containing 200 mM dNTPs, 1 mM sense and antisense primers, 1.25 mM $MgCl_2$, 2 μl 10× PCR buffer, and 0.5 U Taq polymerase (Applied Biosystems, Foster City, CA). The PCR primers used were those listed in the Ref. 39 β-actin was used as the endogenous control. The cycling parameters were as follows: denaturation at 95°C for 45 s, primer annealing at 55°C for 45 s, and 35 cycles of extension at 72°C for 60 s. PCR cycling was preceded by an initial denaturation at 95°C for 5 min, followed by final extension at 72°C for 5 min. The PCR products were analyzed by electrophoresis on a 1.5% agarose gel; this was followed by staining with ethidium bromide. If no signal was observed, the remaining PCR products were amplified by an additional 15 cycles and analyzed again to confirm the absence of the signal.

Quantitative RT-PCR for NY-ESO-1 expression

After synthesis of the first cDNA strand as described earlier, quantitative RT-PCR was performed on the LightCycler real-time RT-PCR system (version 3.39) (Roche, Mannheim, Germany), using the FastStart Taqman Probe Master (ROX) (Roche) along with sets of primers and Universal ProbeLibrary probes (Roche) designed online with ProbeFinder version 2.40 (Roche). Probes specific for NY-ESO-1 were as follows: forward primer: 5′-TGTCCGGCAACATACTGACT-3′, reverse primer: 5′-ACTGCGTGATCCACATCAAC-3′, and Universal ProbeLibrary probe Human No. 67 (Roche), which yields a 111-nt amplicon. The endogenous reference gene *GAPDH* was amplified by the forward primer: 5′-AGCCACATCGCTCAGACAC-3′, reverse primer: 5′-CGCCCAATACGACCAAATC-3′, and Universal ProbeLibrary probe Human No. 60, which yields a 67-nt amplicon. Each sample was amplified as follows: 1 cycle at 95°C for 10 min followed by 40 cycles at 95°C for 15 s and 60°C for 1 min. cDNA from SaOS-2 was used to generate the standard curves for *NY-*

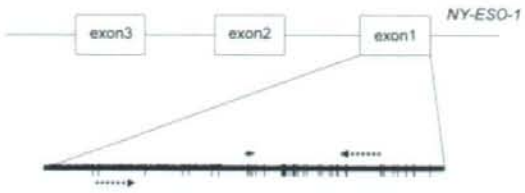

FIGURE 1 – Schematic view of the *NY-ESO-1* gene region analyzed in this study. Vertical lines indicate CpG dinucleotides, the solid arrow indicates the Pyrosequencing primer, and the broken arrows indicate the location of MSP primers.

ESO-1 and *GAPDH*. Standardization of samples was achieved by dividing the copy number of the target gene *NY-ESO-1* by that of the *GAPDH* gene. Values were expressed as ratios relative to *NY-ESO-1* expression in SaOS-2.

Western blot analysis

Cells treated with 5-aza-CdR (1 μM) and untreated cells were lysed in a buffer containing protease inhibitors. Protein samples (45 μg) were denatured at 100°C for 5 min and subsequently applied to each well and electrophoresed on a 12.5% polyacrylamide gel. After transferring the proteins to a polyvinylidene difluoride (PVDF) membrane, it was blocked with 3% low-fat skim milk, incubated with a monoclonal antibody (mAb) against NY-ESO-1 (ES121; Zymed, San Francisco, CA), and then washed and incubated with an horseradish peroxidase (HRP)-labelled secondary Ab. Visualization was performed using an enhanced chemiluminescence technique.

NY-ESO-1 promoter DNA methylation analyses

Methylation-specific PCR (MSP)[40] and Pyrosequencing™ technology[41] were used to determine the methylation status of the CpG island region of *NY-ESO-1*. None of the sequences identified in the *NY-ESO-1* promoter region fulfilled the criteria for CpG islands (length, >200 bp, G + C content, >50%, observed CpG/expected CpG ratio, ≥0.6).[42] The CpG islands and the location of the primers in exon 1 for DNA methylation analyses are shown in Figure 1. Genomic DNA isolation and sodium bisulphite conversion were performed as described previously.[43] The primer sequences and annealing temperatures of MSP were as reported previously.[44] The primer sequences for Pyrosequencing™ were designed using PSQ Assay Design (Biotage, Uppsala, Sweden). A 50-μl PCR was carried out in 60 mM Tris ± HCl (pH 8.5), 15 mM ammonium sulphate, 2 mM $MgCl_2$, 10% DMSO, 1 mM dNTP mix, 1 U Taq polymerase, 5 pmol forward primer (5′-GGGTTGAATGGATGTTGTAG-3′), 50 pmol reverse primer (5′-CRCCACCAAAACTATCAA-3′), 50 pmol biotinylated universal primer (5′- GGGACACCGCTGATCGTTTACRCCACCAAAAC-TATCAA-3′) and ~50 ng bisulphite-treated genomic DNA. The forward primer contains a 20-bp linker sequence on the 5′ end that is recognized by biotin-labeled primera; thus, the final PCR product can be purified using Sepharose beads. PCR cycling conditions were as follows: 95°C for 30 s, 60°C for 45 s and 72°C for 45 s for 55 cycles. The biotinylated PCR product was purified and made single-stranded to act as a template in a pyrosequencing reaction using the Pyrosequencing Vacuum Prep Tool (Pyrosequencing, Westborough, MA), as recommended by the manufacturer. In brief, the PCR product was bound to Streptavidin Sepharose HP (Amersham Biosciences, Uppsala, Sweden), and the Sepharose beads containing the immobilized PCR product were purified, washed, denatured using 0.2 M NaOH solution and washed again. Then, 0.3 mM pyrosequencing primer (5′-TGAATGGATGTTG-TAGATG-3′) was annealed to the purified single-stranded PCR product, and pyrosequencing was performed using the PSQ HS 96Pyrosequencing System (Pyrosequencing). Methylation quantification was performed using the provided software.

Flow cytometric analysis

Glioma cells were treated with 5-aza-CdR as described earlier. The treated and untreated cells were stained with anti-HLA class-I mAbs (W6/32; kindly provided by Dr. K. Itoh, Kurume University, Kurume, Japan) or isotype control mouse IgG2a followed by staining with fluoroscein isothiocyanate (FITC)-labelled anti-mouse IgG Abs. Flow cytometric analysis of stained cells was performed by using FACS Calibur (Becton Dickinson, San Jose, CA).

Induction of HLA-A2-restricted NY-ESO-1-specific CTL lines by peptide-pulsed dendritic cells

Peripheral blood mononuclear cells (PBMCs) from healthy volunteers genetically typed as HLA-A2-positive by SRL, (Tokyo, Japan) were isolated using Ficoll-Paque (Amersham Biosciences). Peptide-pulsed dendritic cells (DCs) were prepared from donor-derived PBMCs, as described previously[37] with minor modifications. In brief, the plastic adherent cells from PBMCs were cultured in AIM-V medium (Life Technologies, Gaithersburg, MD) supplemented with recombinant human granulocyte/macrophage-colony stimulating factor (rhGM-CSF, 500 U/ml) and rhIL-4 (500 U/ml) at 37°C in a humidified CO_2 (5%) incubator. After 6 days, the culture medium was removed, and the immature DCs were cultured in AIM-V supplemented with rhGM-CSF (500 U/ml), recombinant human interleukin (rhIL)-4 (500 U/ml), rhIL-6 (1,000 U/ml), recombinant human tumor necrosis factor-α (10 ng/ml), and IL-1β (10 ng/ml). All cytokines used were purchased from Strathmann Biotech AG, Hanover, Germany. Mature DCs were harvested after another 2 days, resuspended in AIM-V medium at 1×10^6 cells/ml with the peptide (10 μg/ml), and incubated for 4 hr at 37°C. The peptide-pulsed DCs were then treated with mitomycin-C, washed, and finally resuspended in AIM-V medium supplemented with 10% human AB serum. Autologous $CD8^+$ T cells were enriched from PBMCs by using magnetic microbeads (Miltenyi Biotech, Auburn, CA) and were added (1×10^6/well) to the peptide-pulsed DCs (1×10^5/well) in 2 ml AIM-V medium supplemented with 10% human AB serum, 1,000 U/ml rhIL-6, and 10 ng/ml rhIL-12 in each well of 24-well tissue culture plates. On day 7, the lymphocytes were restimulated with mitomycin-C-treated autologous DCs pulsed with peptides in AIM-V medium supplemented with 10% human AB serum, rhIL-2 and rhIL-7 (10 U/ml each). One week later and on a weekly basis thereafter, the responder cells were restimulated with peptide-pulsed DCs in a medium supplemented with rhIL-2 and rhIL-7 (10 U/ml each). The induction of NY-ESO-1-specific CTL lines was attempted 3 times.

CTL assay

The susceptibility of the untreated and 5-aza-CdR-treated U251 glioma cells (HLA-A2) to HLA-A2-restricted NY-ESO-1-specific CTL lines was evaluated by a standard 4-h ^{51}Cr-releasing assay at various (effector:target) E:T ratios. The percentage specific lysis was calculated as follows: 100 × (experimental release − spontaneous release)/(maximum release − spontaneous release).

Cold target inhibition assay

The cold target inhibition assay was performed as described previously.[45] In brief, T2.A2 cells were incubated with the NY-ESO-1 peptide or the irrelevant IL-13Rα2 peptide at a concentration of 10 μM for 1 hr. After extensive washing, the indicated numbers of peptide-loaded cells were incubated with 2×10^4 cytotoxic effector cells for 1 hr, and then 2×10^3 ^{51}Cr-labeled, 5-aza-CdR-treated U251 glioma cells were added to each well. Cytotoxicity was assessed at the E:T ratio of 10:1 as described earlier.

TABLE I – RT-PCR ANALYSIS FOR EXPRESSION OF CANCER-TESTIS ANTIGENS IN GLIOMA TISSUES

Patient	Pathology	NY-ESO-1	MAGE-1	MAGE-3	MAGE-4	MAGE-6	MAGE-10	MAGE-3/6	LAGE-1	CT7	SCP-1	SSX-1	SSX-2	SSX-4
1	GBM		■											
2	GBM													
3	GBM													
4	GBM													
5	GBM							■						
65	GBM													
194	GBM													
195	GBM													
197	GBM													
198	GBM													
199	GBM													
6	AA													
7	AA													
8	AA													
9	AA													
12	AA	■	■				■	■						
14	AA				■									
67	AA													
69	AA													
78	AA													
189	AA													
190	AA													
202	AA													
203	AA													
16	AS													
17	AS													
18	AS													
192	AS													
193	AS													
200	AS													
Rate		(1/30)	(2/30)	(0/30)	(1/30)	(0/30)	(1/30)	(2/30)	(0/30)	(0/30)	(0/30)	(0/30)	(0/30)	(0/30)

We investigated the composite expression of 13 CTAs in 30 human glioma specimens by RT-PCR analysis. MAGE-4, MAGE-10 and NY-ESO-1 were expressed in only 1 sample out of 30, and MAGE-1 and MAGE3/6 were expressed in 2 samples. Other CTAs were all negative in the 30 brain tumor specimens tested. The expression pattern of these did not correlate with the histological grades of gliomas.

Black and white boxes indicate positive and negative expression, respectively.

GBM, glioblastoma multiforme (WHO Grade IV); AA, anaplastic astrocytoma (Grade III); AS, astrocytoma (Grade II).

Orthotopic glioma xenograft model

Female nonobese diabetic/severe combined immunodeficiency disease (NOD/SCID) mice aged 5 weeks were used in the experiments. All mice were purchased from SLC, Hamamatsu, Japan. They were maintained under specific pathogen-free conditions in the animal facility of Nagoya University School of Medicine. Animal experiments were performed according to the principles enunciated in the Guide for the Care and Use of Laboratory Animals prepared by the Office of the Prime Minister of Japan.

Mice were anaesthetized with an intraperitoneal injection of pentobarbital (60–70 mg/kg body weight). After shaving the hair and incising the scalp, a burr hole was made in the skull 3 mm lateral to the midline and 4 mm posterior to the bregma using a dental drill. The head of each mouse was fixed in a stereotactic apparatus with ear bars, and 2×10^5 U251 cells in 2 μl PBS were stereotactically injected over 4 min at a depth of 2 mm below the dura mater. A sterile Hamilton syringe fitted with a 26-gauge needle was used with a microsyringe pump. The needle was retained in the brain for an additional 2-min duration and then slowly withdrawn.

To test the induction of *NY-ESO-1* in orthotopic glioma xenografts, 5-aza-CdR [0.2 mg/kg, intraperitoneally (i.p)] was administered every 12 hr for 4 consecutive days (8 pulses) starting on day 14 after glioma inoculation. The control brain tumor model was treated under similar experimental conditions by an i.p. PBS injection. To determine whether the treated cells upregulated the *NY-ESO-1* expression, the mice were killed on day 3 after the final 5-aza-CdR injection. The brain tumors were removed for RT-PCR for NY-ESO-1.

Tumor-inoculated NOD/SCID mice were randomly divided into 4 treatment groups (10 animals each) to examine the treatment efficacy of NY-ESO-1-specific CTLs in combination with 5-aza-CdR. The animals in the various groups were then injected as follows: Group I, PBS (i.p., 8 pulses starting from the day after tumor inoculation) and PBS (2 μl) intratumorally (i.t.) 6 days after tumor inoculation; Group II, PBS i.p. (8 pulses) and bulk CTLs (i.t., 1×10^6 cells/mouse in 2 μl); Group III, 5-aza-CdR i.p. (0.2 mg/kg, 8 pulses) and PBS (i.t., 2 μl); Group IV, 5-aza-CdR i.p. (0.2 mg/kg, 8 pulses) and bulk CTLs (i.t., 1×10^6 cells/mouse in 2 μl). Five mice in each group were euthanized using CO_2 inhalation on day 21 after tumor injection. The mice were transcardially perfused with 4% paraformaldehyde. The brain tissue was postfixed overnight, embedded in paraffin, and then cut into 5-μm serial horizontal sections. Tissue sections were stained by the standard haematoxylin and eosin technique. The growth inhibitory effect was evaluated by measuring the long (a) and short (b) axes in the coronal section showing the maximal area of each tumor. The approximate volume of the tumor (V) was calculated according to the formula, V (mm^3) = $a \times b^2/2$. In addition, the survival times of all the remaining mice were recorded.

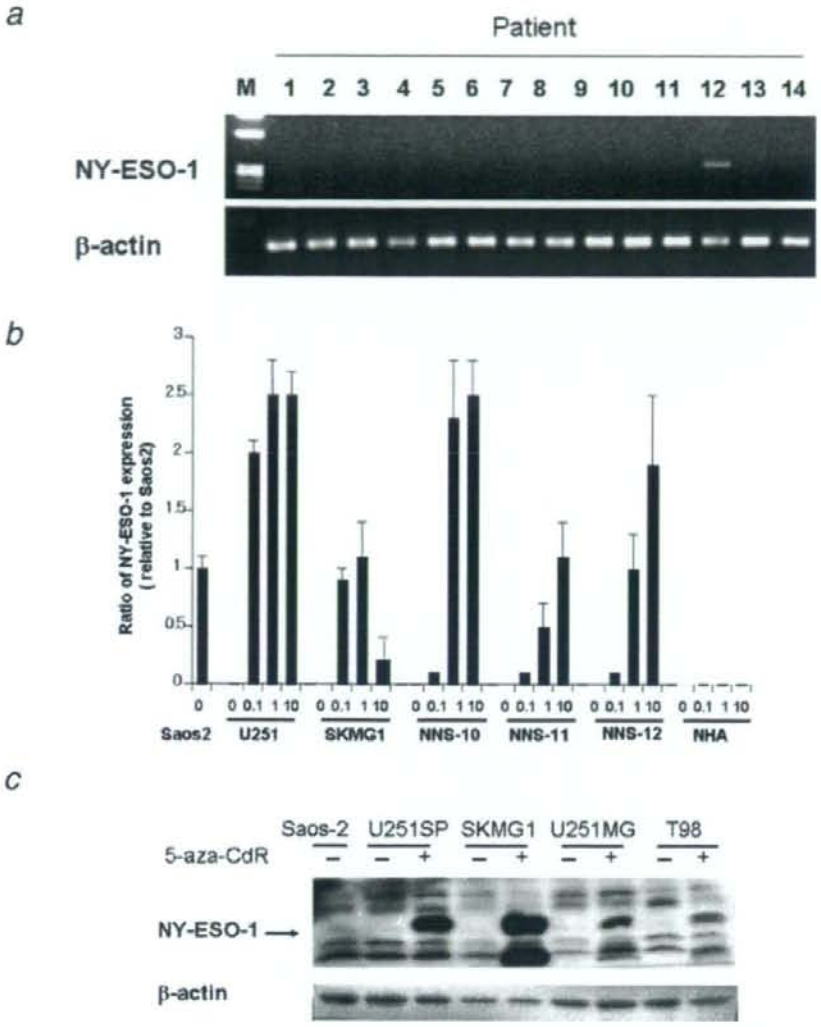

FIGURE 2 – *NY-ESO-1* expression in human gliomas. (*a*) RT-PCR for *NY-ESO-1* in surgical specimens of gliomas. The summarized data is presented in Table I. (*b*) Real-time quantitative RT-PCR showing *NY-ESO-1* induction in glioma cells but not in normal cells by 5-aza-CdR. The expression of *NY-ESO-1* was upregulated in U251, SKMG1, and primary-cultured glioma cells (NNS-10, NNS-11 and NNS-12) treated with 0.1, 1 and 10 μM 5-aza-CdR but not in normal astrocytes (NHA). 5-aza-CdR (10 μM) induced toxicity in SK-MG-1, leading to decreased *NY-ESO-1* expression. (*c*) Detection of NY-ESO-1 in glioma cell lines by western blot analysis. We prepared cell lysates of the untreated (−) gliomas (U251 (sublines SP and MG), SKMG1 and T98) and those treated (+) with 5-aza-CdR (1 μM) and *NY-ESO-1*-positive osteosarcomas (SaOs-2, as a positive control); western blotting analysis was conducted using an anti-NY-ESO-1 mAb.

The statistical significance of the difference in tumor volumes and Kaplan–Meier survival curves was determined by analysis of variance (ANOVA) (StatView, SAS Institute, Cary, NC) with Bonferroni's correction for multiple comparisons and the log-rank test (StatView), respectively.

Results

Expression of individual CTA genes in human gliomas and glioma cell lines

Although the expression frequencies of many CTAs in a variety of neoplasms have been determined, their expression in human gliomas remains unclear, and the expression frequency of CTAs varies drastically among ethnic groups.[39] It would be useful to analyze the expression pattern of CTAs in gliomas in the Japanese population. In our study, RT followed by 35 cycles of amplification revealed that the expression of CTA genes was nearly imperceptible in human gliomas, and the expression pattern of these genes did not correlate with the histological grades of the gliomas (Table I). *MAGE-4*, *MAGE-10* and *NY-ESO-1* were expressed in only 1 of 30 samples, and *MAGE-1* and *MAGE-3/6* were expressed in 2 samples. The samples were negative for *MAGE-3*, *MAGE-6*, *LAGE-1*, *CT7*, *SCP-1*, *SSX-1*, *SSX-2* and *SSX-4* even after 50 amplification cycles of the 30 brain tumor specimens tested (Fig. 2*a* and Table I). Moreover, the human glioma cell lines and primary-cultured glioma cells did not test positive for any of the 13 CTAs even after 50 amplifica-

TABLE II – INDUCTION OF CTA EXPRESSION BY 5-AZA-CDR IN GLIOMA CELLS AND NORMAL CELLS

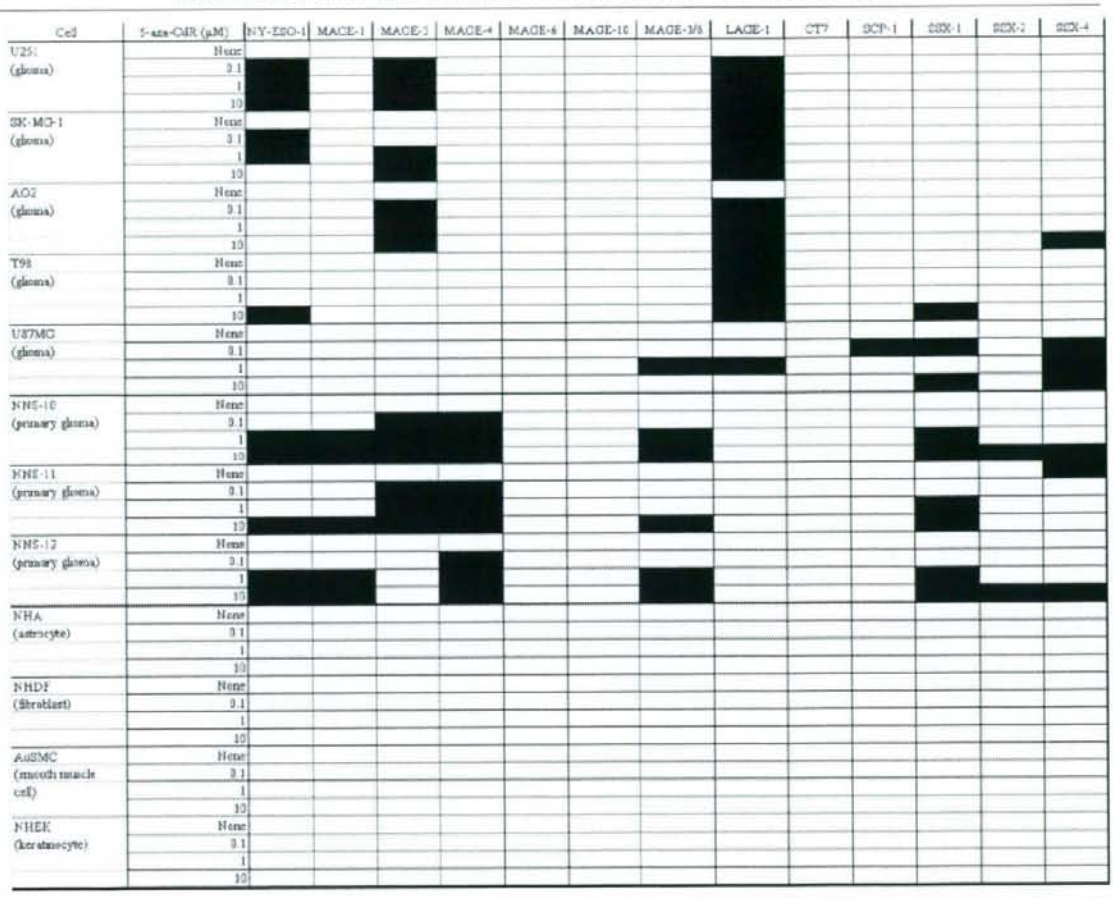

We assessed whether CTAs could be induced by 5-aza-CdR treatment in 5 human glioma cell lines, 3 primary glioma cell lines and 4 human normal cells. The cells were treated with 0.1, 1 and 10 μM 5-aza-CdR every 12 h for 2 consecutive days (4 pulses). The human glioma cell lines and primary-cultured glioma cells did not test positive for any of the 13 CTAs even after 50 amplification cycles. The only exception was *LAGE-1;* SKMG1 and T98 cells constitutively expressed *LAGE-1*. Exposure to 5-aza-CdR invariably induced the expression of *LAGE-1, MAGE-1, MAGE-3, MAGE-4, MAGE-3/6, SCP-1, SSX-1, SSX-2, SSX-4* and *NY-ESO-1* in CTA-negative glioma cells. Because of toxicity, *NY-ESO-1* expression in SK-MG-1, and *MAGE-3/6* and *LAGE-1* expression in U87MG are not observed when treated with 10 μM 5-aza-CdR. In contrast to glioma cells, administration of the agent does not induce CTA expression in human astrocytes, fibroblasts, smooth muscle cells and epidermal keratinocytes.

tion cycles (Table II). The only exception was *LAGE-1*; SKMG1 and T98 cells constitutively expressed *LAGE-1*.

Effect of 5-aza-CdR on glioma cells and normal human cells in vitro

We assessed whether CTAs could be induced by 5-aza-CdR treatment in 5 human glioma cell lines and 3 primary glioma cell lines. The glioma cells were treated with 0.1, 1 and 10 μM 5-aza-CdR every 12 hr for 2 consecutive days (4 pulses). Table II summarizes the expression of the 13 CTA genes detected by RT-PCR in glioma cell lines treated with 0.1, 1 and 10-μM 5-aza-CdR. Exposure to 5-aza-CdR invariably induced the expression of *LAGE-1, MAGE-1, MAGE-3, MAGE-4, MAGE-3/6, SCP-1, SSX-1, SSX-2, SSX-4* and *NY-ESO-1* in CTA-negative glioma cells. Among these, we focused on *NY-ESO-1*-the most immunogenic CTA. Real-time quantitative RT-PCR was performed to quantitate *NY-ESO-1* expression in U251, SK-MG-1 and the primary-cultured glioma cells derived from patients (NNS-10, NNS-11 and NNS-12). These results were then compared with those of the *NY-ESO-1*-expressing SaOS-2 cells (Fig. 2*b*). The expression of *NY-ESO-1* was invariably induced by 5-aza-CdR in all glioma cells tested although the efficiency varied among cells; in particular, 10 μM 5-aza-CdR induced toxicity in SK-MG-1, leading to decreased *NY-ESO-1* expression. Similar toxicity occurred in U87MG cells (Table II).

It is particularly important to ensure that CTA is not induced in normal cells, including normal brain cells, in order to prevent them from being targets of CTA-specific immune responses. We therefore treated human astrocytes, fibroblasts, smooth muscle cells and epidermal keratinocytes with 5-aza-CdR. In contrast to

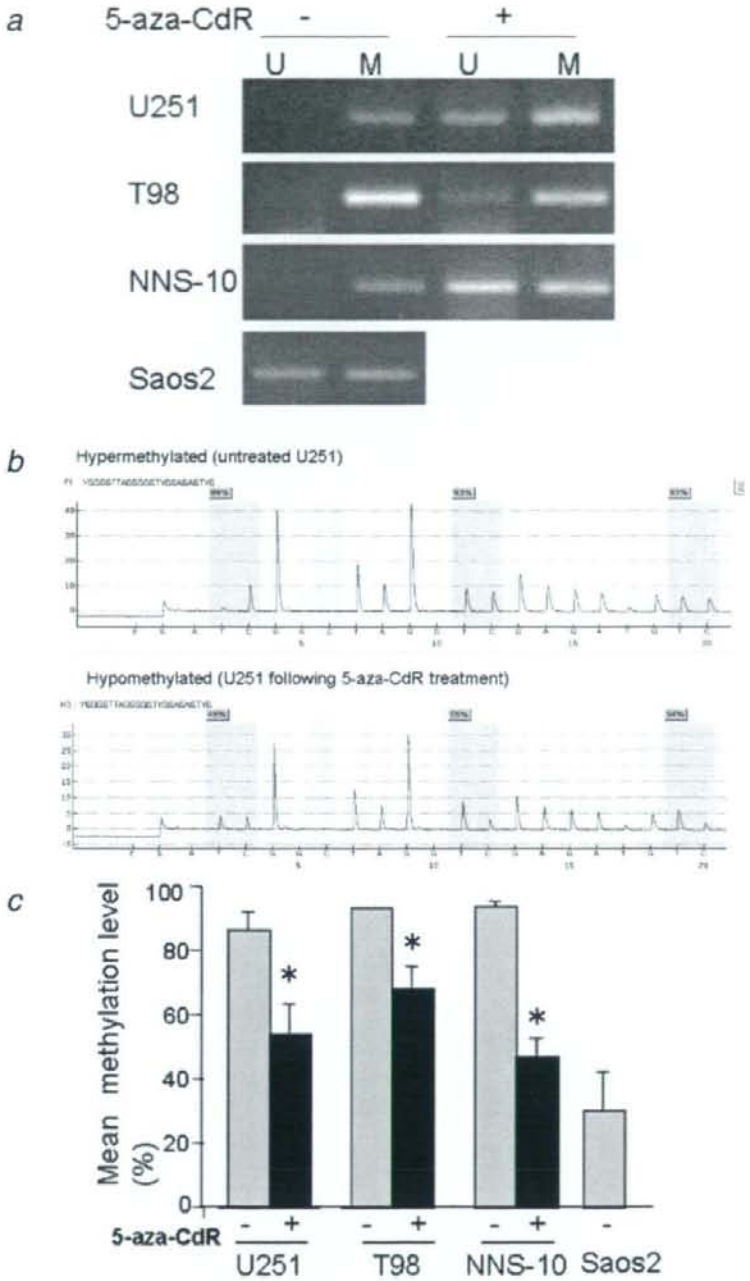

FIGURE 3 – *NY-ESO-1* methylation analyses. (*a*) DNA methylation of the *NY-ESO-1*-gene was measured by MSP. The *NY-ESO-1* is heavily methylated in glioma cells but not in SaOS2 cells before 5-aza-CdR treatment, and it is hypomethylated following 5-aza-CdR exposure. U and M, reactions for unmethylated and methylated sequences, respectively. (*b*) Representative pyrograms of hyper- and hypomethylation. The sequence in the upper part of each pyrogram represents the sequence under investigation. The sequence below the pyrogram indicates the sequentially added nucleotides. The gray regions indicate the analyzed C/T sites; the percentage values for the respective cytosine methylation are provided above them. Yellow regions indicate the positions where a cytosine was added to verify the complete conversion from unmethylated cytosine to thymine. (*c*) Quantitative analyses of NY-ESO-1 methylation by pyrosequencing. Mean methylation levels ± SD were 86.3% ± 5.5%, 93.3% ± 0.6% and 93.3% ± 1.5% for U251, T98 and NNS-10 glioma cells, respectively, while it was 30% ± 12% for SaOS2 cells constitutively expressing NY-ESO-1. Following 5-aza-CdR treatment (+), methylation levels were significantly decreased to 54% ± 9.1%, 68% ± 6.9% and 46.7% ± 5.7% for U251, T98 and NNS-10. * $p < 0.05$ compared to untreated (−) cells. [Color figure can be viewed in the online issue, which is available at www.interscience.wiley.com.]

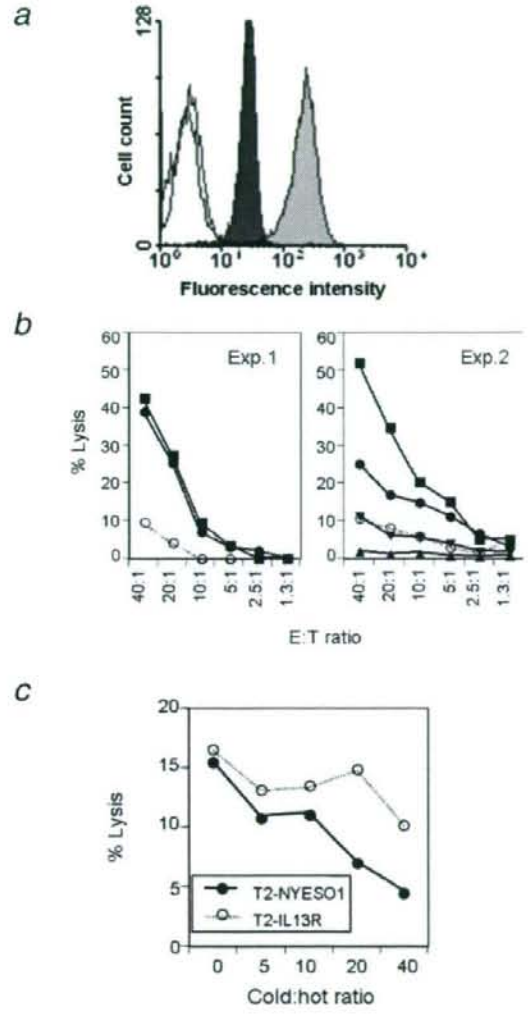

FIGURE 4 – Antigenic potentiation of glioma cells by 5-aza-CdR. (*a*) Upregulation of HLA class I. Untreated U251 glioma cells (black) and those treated with 5-aza-CdR (gray) were stained with anti-HLA class I mAbs (W6/32). Negative staining of untreated and treated U251 cells with isotype control mouse IgG2a is shown (white). (*b*) Cytolytic activity of 2 independently induced NY-ESO-1 CTL lines against U251 (HLA-A2$^+$) before (○) and after (●) 5-aza-CdR treatment; other NY-ESO-1$^-$ glioma cells, SK-MG-1 (A24, ▲); human osteosarcoma cells, SaOS-2 (A2, NY-ESO-1$^+$, ■); and human myeloid leukaemia cell line K562 (▼). Exp. 1, Experiment 1; Exp. 2, Experiment 2. (*c*) The CTL-mediated target cell (5-aza-CdR-treated U251) lysis was blocked using T2.A2 cells that had been loaded with the HLA-A2-binding NY-ESO-1 peptide p157-165 (SLLMWITQC) (●) but not with the control peptide, *i.e.*, the HLA-A2-binding IL-13Rα2 peptide p345-354 (WLPFGFILI) (○). The same CTL line as in the Exp. 2 of Figure 4*b* was used in the experiment (E:T ratio, 10:1).

glioma cells, administration of the agent did not induce CTA expression in these cells (Fig. 2*b* and Table II).

To assess whether the induction of CTA mRNA is followed by the production of the appropriate protein, western blotting for NY-ESO-1 was performed using untreated and 5-aza-CdR-treated glioma cell lines. The SaOS-2 osteosarcoma cell line, which constitutively expresses *NY-ESO-1* without 5-aza-CdR treatment, was used as a positive control. As shown in Figure 2*c*, 23-kDa bands corresponding to NY-ESO-1 were observed in all glioma cell lines treated with 5-aza-CdR but were absent in the untreated cells (all data not shown). This result suggested that the *NY-ESO-1* expression was induced after 5-aza-CdR treatment at the protein level as well as the mRNA level.

Quantitative CpG island mapping with Pyrosequencing™

MSP experiments were performed to evaluate the methylation status of *NY-ESO-1* in cultured glioma cells. We observed that the *NY-ESO-1* is heavily methylated in glioma cells before 5-aza-CdR treatment and becomes hypomethylated following 5-aza-CdR exposure (Fig. 3*a*). To quantify the methylation of the CpG sites of *NY-ESO-1*, we employed a novel real-time DNA sequencing technology called Pyrosequencing™. This technology was originally developed for the analysis of single-base variations and enables the precise quantification of incorporated nucleotides at polymorphic positions. Treatment of the DNA with sodium bisulphite converts the epigenetic difference between methylated and unmethylated cytosine into a single-base variation of the C/T type. Therefore, Pyrosequencing is a very suitable tool for methylation analysis. Representative pyrograms for hypermethylated (untreated U251 cells) and hypomethylated (U251 cells following 5-aza-CdR exposure) are shown in Figure 3*b*. We identified the regions showing the largest differences in methylation and compared methylation levels of a small window (3 CpG sites) of *NY-ESO-1*. Mean methylation levels ± standard deviation (SD) were 86.3% ± 5.5%, 93.3% ± 0.6% and 93.3% ± 1.5%, for U251, T98 and NNS-10 glioma cells, respectively, while it was 30% ± 12% for SaOS2 cells constitutively expressing *NY-ESO-1*. Following 5-aza-CdR treatment, methylation levels were significantly decreased to 54% ± 9.1%, 68% ± 6.9% and 46.7% ± 5.7% for U251, T98 and NNS-10 ($p < 0.05$) (Fig. 3*c*). The MSP and Pyroseqencing data of other glioma cell lines and primary glioma cells were almost identical (data not shown). Taken together, this result is consistent with the hypothesis that 5-aza-CdR mediated NY-ESO-1 activation is a consequence of DNA demethylation.

Upregulation of HLA class I in glioma cells

Our microarray data (supplemental data and Discussion) indicated that HLA class I molecules can be upregulated by ~3-fold (Table SII). Flow cytometric analysis confirmed that HLA class I expression was significantly increased in the 5-aza-CdR-treated glioma cells when compared to that in the untreated cells, indicating that 5-aza-CdR could affect the constitutive expression of HLA class I antigens in gliomas. The representative data of U251 cells are shown in Figure 4*a*. Combined with the analyses on the effect of 5-aza-CdR on *NY-ESO-1* expression, our study suggests that 5-aza-CdR may have potential therapeutic implications in *NY-ESO-1*-specific immunotherapy for human gliomas.

Antigenicity of forcibly expressed NY-ESO-1 in glioma cells by 5-aza-CdR

To evaluate the antigenicity of forcibly expressed *NY-ESO-1*, HLA-A2-restricted *NY-ESO-1*-specific CTL lines were generated, and their cytotoxicity against 5-aza-CdR-treated glioma cells was tested. Cytotoxic activity was observed only in SaOS-2 osteosarcoma cells (*NY-ESO-1*+ and HLA-A2) and 5-aza-CdR-treated U251 glioma cells, depending on the E:T ratios (Fig. 4*b*). In contrast, untreated U251 cells and other glioma cells (*NY-ESO-1*-negative and HLA-A2-negative) were resistant to lysis. K562 cells were included in order to assess the degree of the natural-killer activity of the CTL cultures; this activity was found to be negligible. Cold target inhibition assays demonstrated that cytotoxicity against 5-aza-CdR-treated U251 cells was specifically inhibited in the presence of T2.A2 cells that were prepulsed with the cognate but not those that were prepulsed with an irrelevant peptide (Fig. 4*c*). This indicated that CTL lines recognized the NY-ESO-1 pep-

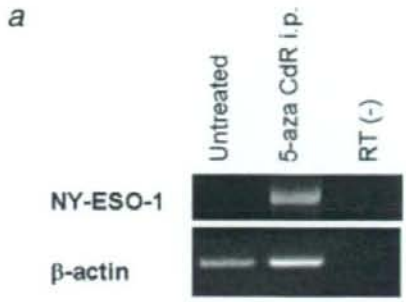

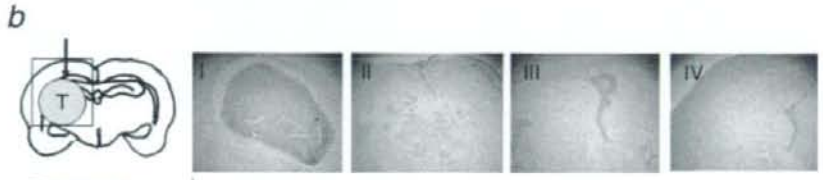

Treatment				
i.p.	PBS	PBS	5-aza-CdR	5-aza-CdR
i.t.	PBS	CTL	PBS	CTL
Tumor volume (Mean±SD mm3)	32.2± 8.4	27.5 ± 8.9	12.2 ± 4.1	8.1 ± 2.5*

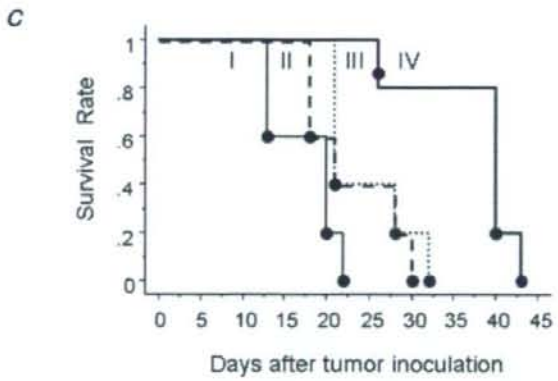

FIGURE 5 – Therapeutic effects of the adoptive transfer of NY-ESO-1-specific CTLs and 5-aza-CdR treatment in the human glioma orthotopic xenograft model. (*a*) RT-PCR for NY-ESO-1 in intracerebral glioma after i.p. injection of 5-aza-CdR. (*b*) Histopathological characteristics (haematoxylin and eosin, magnification: 40×) and tumor volumes of animals treated with PBS i.p. (8 pulses from the day after tumor inoculation) and PBS (2 μl) i.t. 6 days after tumor inoculation (Group I), PBS i.p. (8 pulses) and NY-ESO-1-specific bulk CTLs (1×10^6 cells/mouse in 2 μl) i.t. (Group II), 5-aza-CdR i.p. (0.2 mg/kg, 8 pulses) and PBS (2 μl) i.t. (Group III), or 5-aza-CdR i.p. (0.2 mg/kg, 8 pulses) and NY-ESO-1-specific bulk CTLs (1×10^6 cells/mouse in 2 μl) i.t. (Group IV). The mean tumor volume + SD in each group is shown in the table. The schema of brain coronal section shows the tumor (T), the injection site of CTL/PBS (arrow), and the magnified area (box). * $p < 0.05$ compared to other 3 treatment groups. (*c*) Kaplan–Meier survival curves of groups I–IV. The survival time of mice treated with 5-aza-CdR and NY-ESO-1-specific CTLs was significantly greater than that of mice in Groups I, II and III ($p = 0.0019$, 0.0126 and 0.0132, respectively).

tides that were processed and presented. These results together indicated that the amount of 5-aza-CdR-induced NY-ESO-1 in glioma cells was sufficient to render them sensitive to HLA-A2-restricted *NY-ESO-1*-specific CTLs *in vitro*.

Induction of NY-ESO-1 expression in intracerebral glioma by systemic administration of 5-aza-CdR

Previous evidence indicates that 5-aza-CdR can cross the BBB effectively, maintaining cytotoxic concentrations in the cerebrospinal fluid when administered *via* continuous intravenous infusion.[46] To evaluate whether *NY-ESO-1* expression could be induced *in vivo* after systemic delivery of 5-aza-CdR, we employed NOD/SCID mice transplanted intracerebrally with U251 glioma cells (NY-ESO-1 negative). After the mice were injected i.p. with a 0.2 mg/kg dose of 5-aza-CdR at 12 hr intervals for 4 days, the tumors were resected and subjected to RT-PCR analysis for *NY-ESO-1*. The results demonstrated that *NY-ESO-1* expression could be detected in intracerebral gliomas i.p. treated with 5-aza-CdR (Fig. 5*a*).

Growth suppression of glioblastoma xenografts after the adoptive transfer of anti-NY-ESO-1 CTLs

Next, we addressed whether adoptively transferred NY-ESO-1-specific CTLs posses cytotoxic activity against gliomas in which NY-ESO-1 was induced *in vivo* by 5-aza-CdR. In this model, U251 tumor cells were stereotactically implanted in the forebrain of NOD/SCID animals. An intraperitoneal injection of 5-aza-CdR (or PBS) was initiated from the next day for 4 consecutive days at 12-hr intervals. On day 6 after the tumor inoculation, the mice were treated by stereotactic delivery of either NY-ESO-1-specific bulk CTLs or PBS. On day 21 after the tumor inoculation, tumor volumes were evaluated in half of the animals. Tumor growth was significantly delayed in the animals that were administered both 5-aza-CdR (i.p) and CTLs (Group IV), whereas relatively larger tumors were observed in the other 3 groups (Groups I, II and III, $p < 0.05$) (Fig. 5*b*). In addition, we measured the survival of the remaining half of the animals. The Kaplan–Meier survival curves of 4 groups are shown in Figure 5c. The survival time of mice treated with 5-aza-CdR and NY-ESO-1-specific CTLs was significantly greater than that of mice in Groups I, II and III ($p = 0.0019$, 0.0126 and 0.0132, respectively). Interestingly, 5-aza-CdR injection alone (Group III) exerted a beneficial antitumor effect in terms of tumor volumes and survival ($p < 0.05$ *vs.* Group I). As discussed later, the formation of enzyme-DNA adducts mediated by *p53* induction may account for the efficacy and toxicity of 5-aza-CdR *in vivo*.

Discussion

The principal findings of this study are that in spite of relatively low frequency of CTA expression in gliomas, the DNA demethylating agent 5-aza-CdR remarkably induced the expression of CTAs, including NY-ESO-1-one of the most immunogenic CTAs-in glioma cells but not in normal human cells. The de novo expressed NY-ESO-1 was effectively recognized by the specific CTL lines both *in vitro* and in glioma orthotopic xenografts.

Expression of CTAs in human gliomas

A German group investigated the expression of 7 CTAs (SSX-1, SSX-2, SSX-4, SCP-1, TS85, NY-ESO-1 and MAGE-3) in 50 gliomas by RT-PCR. They demonstrated that SCP-1 was most frequently positive (40%), followed by SSX-4 (27%) and MAGE-3 (7%).[35] However, the expression frequency of CTAs in gliomas remains unclear, particularly when focusing on different ethnic groups. For example, NY-ESO-1 and LAGE-1 are expressed at much lower frequencies in lung cancer in the Japanese than in Caucasians; NY-ESO-1 is expressed in 2% of the Japanese *versus* 17 or 20% in Caucasians, and LAGE-1 is expressed in 9% of the Japanese *versus* 33% expression in Caucasians.[39] Liu *et al.*, have reported MAGE-1 expression in approximately 40% of glioblastoma primary cell lines and in established glioma cell lines, including U87MG, which is inconsistent with our results.[47] Although the reasons for the inconsistency remain unclear, the differences in ethnic groups and culture conditions (*e.g.*, passage and confluency) might be responsible. Nevertheless, overall, we found that gliomas have a very low frequency of CTA gene expression, such as NY-ESO-1, indicating that brain tumors are considerably unsuitable for CTA-based immunotherapy. To overcome this limitation, novel CTA induction strategies are required to evoke strong immune responses against gliomas.

CTA as targets of demethylation

A cascade of biochemical events for gene silencing is triggered by CpG island methylation that involves DNA methyltransferase activity, which in turn attracts histone deacetylases and histone methylases that eventually modify histones into a silenced chromatin state.[48] The agent 5-aza-CdR has been shown to interrupt this silencing cascade effectively by binding covalently to DNA methyltransferase and inhibiting its enzymatic activity. Numerous studies have shown the ability of 5-aza-CdR to reactivate the transcription of several tumor suppressor genes (*i.e. p16* and *MGMT*) in human tumors.[28,29] Previous evidence has clearly defined the regulatory role of DNA methylation in the constitutive expression of CTAs in melanomas and renal cell carcinomas and has demonstrated that *in vitro* treatment with 5-aza-CdR induces their expression in neoplastic cells. Therefore, CTAs are intriguing targets for demethylation. Here, we studied a large panel of CTAs and showed that 5-aza-CdR reactivated the expression of a variety of CTAs in human gliomas. This result is consistent with the report of Liu *et al.*, showing that 5-aza-CdR induced the mRNA expression of MAGE-1.[47] Then, we determined whether 5-aza-CdR-mediated NY-ESO-1 activation is a consequence of promoter DNA methylation by using MSP and quantitative Pyrosequencing. Although MSP is very sensitive and easy to use, it does not provide precise information about the methylation status of single CpG sites. Recently, Pyrosequencing technology was developed for the analysis of single-base variations. An indirect bioluminometric assay quantitatively measures the amount of pyrophosphate (Ppi) that is released from each incorporated dNTP. Through an enzymatic cascade, the release is converted into a light signal that is directly proportional to the amount of incorporated dNTP, appearing as peaks in a Pyrogram. Employing this technology, we first showed that only a small region of the *NY-ESO-1* CpG island provides relevant information for differential methylation analysis.

Expression profiling and gene ontology analysis after 5-aza-CdR treatment

To identify alterations in gene expression after 5-aza-CdR treatment, we conducted microarray experiments (supplementary data). Once the analysis was completed, we narrowed down the number of potential targets by selecting only those genes whose expression changed more than 2-fold in 2 independent RNA preparations. A total of 65 genes that fulfilled our criteria were upregulated, and 24 genes were downregulated following 5-aza-CdR treatment (Table SII). To identify the biological processes significantly involved in the drug effect, genes considered differentially expressed between the treated and control glioma cells were processed through the Gene Ontology (GO) program. The majority of the differentially expressed genes were related to biological process categories such as apoptosis (programmed cell death), cell proliferation, immune system process and tissue development (Table SIII). These categorized GO terms supported the fact that DNA methylation is associated with various biological epigenetic processes, including cell differentiation, development and oncogenic transformation. For the 11 upregulated genes underlined in Supplementary Table SII, we confirmed the microarray data using semiquantitative RT-PCR with the primers listed in Supplementary Table SIV on the same glioma cell line (U251) and 3 others (AO2, T98 and SKMG1). As shown in Supplementary Figure S1, we were able to show marked up-regulation of the tissue inhibitor of metalloprotease (TIMP) gene, which has been found to be silenced by aberrant promoter hypermethylation in other tumor types,[49] thus validating our screening procedures. Interestingly, p53, Gadd45, NF-κB and caspase 4 genes were activated by 5-aza-CdR, although the dose of 5-aza-CdR in this study (1 μM) did not affect the cell viability and morphology in glioma cells (data not shown). Recently, Kim *et al.*, attempted to identify genes silenced epigenetically in malignant gliomas by using a comprehensive and intense microarray technique coupled with the inhibition of DNA methylation and histone deacetylation.[50] Although they validated the reactivation of the MAGE genes in their micoarray screen, they mainly focused on novel targets harbouring the CpG island promoter. In addition to the role of 5-aza-CdR in the activation of epigenetically silenced genes, an important biological activity of this agent is the formation of enzyme-DNA adducts.[51] Karpf *et al.*, reported that the formation of covalent enzyme-DNA adducts and cellular toxicity resulted from the activation of *p53* as a cellular response to DNA damage.[52]

5-Aza-CdR as a potent immunostimulator

Our microarray data (Supplementary data) and the flow cytometric analysis showed that HLA class I expression was significantly increased in the 5-aza-CdR-treated glioma cells. In addition, the efficient recognition of 5-aza-CdR-treated U251 glioma cells by the HLA-A2 restricted NY-ESO-1 specific CTL lines demonstrated that de novo synthesized NY-ESO-1 antigen is functionally processed and presented. Thus, CTL-mediated lysis of glioma cells induced by 5-aza-CdR appears to represent a direct consequence of immunogenic peptides derived from *de novo* expressed NY-ESO-1 and loaded onto upregulated HLA class I molecules. Our *in vivo* study suggested that systemic administration of 5-aza-CdR may be useful in reverting the CTA-negative phenotype of gliomas through the Blood-Brain-Barrier. This evidence strongly identifies 5-aza-CdR as a potential pharmacological agent in designing and establishing new therapeutic strategies in combination with CTA-based immunotherapeutic approaches for glioma patients.

Acknowledgements

The authors thank Mr. Shigeru Saito (Infocom Corporation, Tokyo, Japan) for bioinformatics assistance in Gene Ontology analysis. They also thank Mr. Mitsuo Kihira (Division of Pathology, Kariya Toyota General Hospital, Aichi, Japan) for assistance in the histological study.

References

1. Chen YT, Scanlan MJ, Sahin U, Tureci O, Gure AO, Tsang S, Williamson B, Stockert E, Pfreundschuh M, Old LJ. A testicular antigen aberrantly expressed in human cancers detected by autologous antibody screening. Proc Natl Acad Sci USA 1997;94:1914–18.
2. Boon T, Cerottini JC, Van den Eynde B, van der Bruggen P, Van Pel A. Tumor antigens recognized by T lymphocytes. Annu Rev Immunol 1994;12:337–65.
3. van der Bruggen P, Traversari C, Chomez P, Lurquin C, De Plaen E, Van den Eynde B, Knuth A, Boon T. A gene encoding an antigen recognized by cytolytic T lymphocytes on a human melanoma. Science 1991;254:1643–7.
4. Gure AO, Tureci O, Sahin U, Tsang S, Scanlan MJ, Jager E, Knuth A, Pfreundschuh M, Old LJ, Chen YT. SSX: a multigene family with several members transcribed in normal testis and human cancer. Int J Cancer 1997;72:965–71.
5. Jager D, Unkelbach M, Frei C, Bert F, Scanlan MJ, Jager E, Old LJ, Chen YT, Knuth A. Identification of tumor-restricted antigens NY-BR-1. SCP-1, and a new cancer/testis-like antigen. NW-BR-3 by serological screening of a testicular library with breast cancer serum. Cancer Immun 2002;2:5.
6. Hubank M, Schatz DG. Identifying differences in mRNA expression by representational difference analysis of cDNA. Nucleic Acids Res 1994;22:5640–8.
7. Brinkmann U, Vasmatzis G, Lee B, Yerushalmi N, Essand M, Pastan I. PAGE-1, an X chromosome-linked GAGE-like gene that is expressed in normal and neoplastic prostate, testis, and uterus. Proc Natl Acad Sci USA 1998;95:10757–62.
8. Lucas S, De Plaen E, Boon T. MAGE-B5, MAGE-B6, MAGE-C2, and MAGE-C3: four new members of the. MAGE family with tumor-specific expression. Int J Cancer 2000;87:55–60.
9. Scanlan MJ, Altorki NK, Gure AO, Williamson B, Jungbluth A, Chen YT, Old LJ. Expression of cancer-testis antigens in lung cancer: definition of bromodomain testis-specific gene (BRDT) as a new CT gene. CT9. Cancer Lett 2000;150:155–64.
10. Jager E, Nagata Y, Gnjatic S, Wada H, Stockert E, Karbach J, Dunbar PR, Lee SY, Jungbluth A, Jager D, Arand M, Ritter G, et al. Monitoring CD8 T cell responses to NY-ESO-1: correlation of humoral and cellular immune responses. Proc Natl Acad Sci USA 2000;97:4760–5.
11. Choi JH, Kwon HJ, Yoon BI, Kim JH, Han SU, Joo HJ, Kim DY. Expression profile of histone deacetylase 1 in gastric cancer tissues. Jpn J Cancer Res 2001;92:1300–4.
12. Jones PA, Takai D. The role of DNA methylation in mammalian epigenetics. Science 2001;293:1068–70.
13. Jones PA, Baylin SB. The fundamental role of epigenetic events in cancer. Nat Rev Genet 2002;3:415–28.
14. Eden A, Gaudet F, Waghmare A, Jaenisch R. Chromosomal instability and tumors promoted by DNA hypomethylation. Science 2003; 300:455.
15. Gaudet F, Hodgson JG, Eden A, Jackson-Grusby L, Dausman J, Gray JW, Leonhardt H, Jaenisch R. Induction of tumors in mice by genomic hypomethylation. Science 2003;300:489–92.
16. Bariol C, Suter C, Cheong K, Ku SL, Meagher A, Hawkins N, Ward R. The relationship between hypomethylation and CpG island methylation in colorectal neoplasia. Am J Pathol 2003;162:1361–71.
17. Lin CH, Hsieh SY, Sheen IS, Lee WC, Chen TC, Shyu WC, Liaw YF. Genome-wide hypomethylation in hepatocellular carcinogenesis. Cancer Res 2001;61:4238–43.
18. Narayan A, Ji W, Zhang XY, Marrogi A, Graff JR, Baylin SB, Ehrlich M. Hypomethylation of pericentromeric DNA in breast adenocarcinomas. Int J Cancer 1998;77:833–8.
19. dos Santos NR, Torensma R, de Vries TJ, Schreurs MW, de Bruijn DR, Kater-Baats E, Ruiter DJ, Adema GJ, van Muijen GN, van Kessel AG. Heterogeneous expression of the SSX cancer/testis antigens in human melanoma lesions and cell lines. Cancer Res 2000;60:1654–62.
20. Missiaglia E, Donadelli M, Palmieri M, Crnogorac-Jurcevic T, Scarpa A, Lemoine NR. Growth delay of human pancreatic cancer cells by methylase inhibitor 5-aza-2′-deoxycytidine treatment is associated with activation of the interferon signalling pathway. Oncogene 2005;24:199–211.
21. Momparler RL, Ayoub J. Potential of 5-aza-2′-deoxycytidine (Decitabine) a potent inhibitor of DNA methylation for therapy of advanced non-small cell lung cancer. Lung Cancer 2001;34(Suppl 4):S111–S115.
22. Jackson-Grusby L, Laird PW, Magge SN, Moeller BJ, Jaenisch R. Mutagenicity of 5-aza-2′-deoxycytidine is mediated by the mammalian DNA methyltransferase. Proc Natl Acad Sci USA 1997;94:4681–5.
23. Santi DV, Norment A, Garrett CE. Covalent bond formation between a DNA-cytosine methyltransferase and DNA containing 5-azacytosine. Proc Natl Acad Sci USA 1984;81:6993–7.
24. Santini V, Kantarjian HM, Issa JP. Changes in DNA methylation in neoplasia: pathophysiology and therapeutic implications. Ann Intern Med 2001;134:573–86.
25. Samlowski WE, Leachman SA, Wade M, Cassidy P, Porter-Gill P, Busby L, Wheeler R, Boucher K, Fitzpatrick F, Jones DA, Karpf AR. Evaluation of a 7-day continuous intravenous infusion of decitabine: inhibition of promoter-specific and global genomic DNA methylation. J Clin Oncol 2005;23:3897–905.
26. Wijermans P, Lubbert M, Verhoef G, Bosly A, Ravoet C, Andre M, Ferrant A. Low-dose 5-aza-2′-deoxycytidine, a DNA hypomethylating agent, for the treatment of high-risk myelodysplastic syndrome: a multicenter phase II study in elderly patients. J Clin Oncol 2000; 18:956–62.
27. Kantarjian H, Issa JP, Rosenfeld CS, Bennett JM, Albitar M, DiPersio J, Klimek V, Slack J, de Castro C, Ravandi F, Helmer R, III, Shen L, et al. Decitabine improves patient outcomes in myelodysplastic syndromes: results of a phase III randomized study. Cancer 2006;106: 1794–803.
28. Coral S, Sigalotti L, Altomonte M, Engelsberg A, Colizzi F, Cattarossi I, Maraskovsky E, Jager E, Seliger B, Maio M. 5-aza-2′-deoxycytidine-induced expression of functional cancer testis antigens in human renal cell carcinoma: immunotherapeutic implications. Clin Cancer Res 2002;8:2690–5.
29. Coral S, Sigalotti L, Gasparollo A, Cattarossi I, Visintin A, Cattelan A, Altomonte M, Maio M. Prolonged upregulation of the expression of HLA class I antigens and costimulatory molecules on melanoma cells treated with 5-aza-2′-deoxycytidine (5-AZA-CdR). J Immunother 1999;22:16–24.
30. Schwechheimer K, Laufle RM, Schmahl W, Knodlseder M, Fischer H, Hofler H. Expression of neu/c-erbB-2 in human brain tumors. Hum Pathol 1994;25:772–80.
31. Hiesiger EM, Hayes RL, Pierz DM, Budzilovich GN. Prognostic relevance of epidermal growth factor receptor (EGF-R) and c-neu/erbB2 expression in glioblastomas (GBMs). J Neurooncol 1993;16:93–104.
32. Chi DD, Merchant RE, Rand R, Conrad AJ, Garrison D, Turner R, Morton DL, Hoon DS. Molecular detection of tumor-associated antigens shared by human cutaneous melanomas and gliomas. Am J Pathol 1997;150:2143–52.
33. Scarcella DL, Chow CW, Gonzales MF, Economou C, Brasseur F, Ashley DM. Expression of MAGE and GAGE in high-grade brain tumors: a potential target for specific immunotherapy and diagnostic markers. Clin Cancer Res 1999;5:335–41.
34. Rimoldi D, Romero P, Carrel S. The human melanoma antigen-encoding gene. MAGE-1, is expressed by other tumour cells of neuroectodermal origin such as glioblastomas and neuroblastomas. Int J Cancer 1993;54:527–8.
35. Sahin U, Koslowski M, Tureci O, Eberle T, Zwick C, Romeike B, Moringlane JR, Schwechheimer K, Feiden W, Pfreundschuh M. Expression of cancer testis genes in human brain tumors. Clin Cancer Res 2000;6:3916–22.

36. Debinski W, Gibo DM, Hulet SW, Connor JR, Gillespie GY. Receptor for interleukin 13 is a marker and therapeutic target for human high-grade gliomas. Clin Cancer Res 1999;5:985–90.
37. Okano F, Storkus WJ, Chambers WH, Pollack IF, Okada H. Identification of a novel HLA-A*0201-restricted, cytotoxic T lymphocyte epitope in a human glioma-associated antigen, interleukin 13 receptor α2 chain. Clin Cancer Res 2002;8:2851–5.
38. Jager E, Chen YT, Drijfhout JW, Karbach J, Ringhoffer M, Jager D, Arand M, Wada H, Noguchi Y, Stockert E, Old LJ, Knuth A. Simultaneous humoral and cellular immune response against cancer-testis antigen NY-ESO-1: definition of human histocompatibility leukocyte antigen (HLA)-A2-binding peptide epitopes. J Exp Med 1998;187:265–70.
39. Tajima K, Obata Y, Tamaki H, Yoshida M, Chen YT, Scanlan MJ, Old LJ, Kuwano H, Takahashi T, Takahashi T, Mitsudomi T. Expression of cancer/testis (CT) antigens in lung cancer. Lung Cancer 2003;42:23–33.
40. Herman JG, Graff JR, Myohanen S, Nelkin BD, Baylin SB. Methylation-specific PCR: a novel PCR assay for methylation status of CpG islands. Proc Natl Acad Sci USA 1996;93:9821–6.
41. Colella S, Shen L, Baggerly KA, Issa JP, Krahe R. Sensitive and quantitative universal Pyrosequencing methylation analysis of CpG sites. Biotechniques 2003;35:146–50.
42. Gardiner-Garden M, Frommer M. CpG islands in vertebrate genomes. J Mol Biol 1987;196:261–82.
43. Natsume A, Ishii D, Wakabayashi T, Tsuno T, Hatano H, Mizuno M, Yoshida J. IFN-β down-regulates the expression of DNA repair gene MGMT and sensitizes resistant glioma cells to temozolomide. Cancer Res 2005;65:7573–9.
44. James SR, Link PA, Karpf AR. Epigenetic regulation of X-linked cancer/germline antigen genes by DNMT1 and DNMT3b. Oncogene 2006;25:6975–85.
45. Arai J, Yasukawa M, Ohminami H, Kakimoto M, Hasegawa A, Fujita S. Identification of human telomerase reverse transcriptase-derived peptides that induce HLA-A24-restricted antileukemia cytotoxic T lymphocytes. Blood 2001;97:2903–7.
46. Chabot GG, Rivard GE, Momparler RL. Plasma and cerebrospinal fluid pharmacokinetics of 5-Aza-2′-deoxycytidine in rabbits and dogs. Cancer Res 1983;43:592–7.
47. Liu G, Ying H, Zeng G, Wheeler CJ, Black KL, Yu JS. HER-2, gp100, and MAGE-1 are expressed in human glioblastoma and recognized by cytotoxic T cells. Cancer Res 2004;64:4980–6.
48. Jaenisch R, Bird A. Epigenetic regulation of gene expression: how the genome integrates intrinsic and environmental signals. Nat Genet 2003;33(Suppl):245–54.
49. Ivanova T, Vinokurova S, Petrenko A, Eshilev E, Solovyova N, Kisseljov F, Kisseljova N. Frequent hypermethylation of 5′ flanking region of TIMP-2 gene in cervical cancer. Int J Cancer 2004;108:882–6.
50. Kim TY, Zhong S, Fields CR, Kim JH, Robertson KD. Epigenomic profiling reveals novel and frequent targets of aberrant DNA methylation-mediated silencing in malignant glioma. Cancer Res 2006;66:7490–501.
51. Ferguson AT, Vertino PM, Spitzner JR, Baylin SB, Muller MT, Davidson NE. Role of estrogen receptor gene demethylation and DNA methyltransferase.DNA adduct formation in 5-aza-2′deoxycytidine-induced cytotoxicity in human breast cancer cells. J Biol Chem 1997;272:32260–6.
52. Karpf AR, Moore BC, Ririe TO, Jones DA. Activation of the p53 DNA damage response pathway after inhibition of DNA methyltransferase by 5-aza-2′-deoxycytidine. Mol Pharmacol 2001;59:751–7.

Epstein–Barr virus nuclear antigen 1-specific CD4+ T cells directly kill Epstein–Barr virus-carrying natural killer and T cells

Ayako Demachi-Okamura,[1] Yoshinori Ito,[2] Yoshiki Akatsuka,[1] Kunio Tsujimura,[3] Yasuo Morishima,[4] Toshitada Takahashi[5] and Kiyotaka Kuzushima[1,6,7]

[1]Division of Immunology, Aichi Cancer Center Research Institute, Nagoya; [2]Department of Pediatrics, Nagoya University Graduate School of Medicine, Nagoya; [3]Department of Infectious Diseases, Hamamatsu University School of Medicine, Hamamatsu; [4]Department of Cell Therapy, Aichi Cancer Center Hospital, Nagoya; [5]Aichi Comprehensive Health Science Center, Aichi Health Promotion Foundation, Chita-gun; [6]Department of Cellular Oncology, Nagoya University Graduate School of Medicine, Nagoya, Japan

(Received February 24, 2008/Revised April 1, 2008/Accepted April 1, 2008/Online publication July 29, 2008)

Epstein–Barr virus (EBV) nuclear antigen (EBNA)1 is expressed in every EBV-infected cell, regardless of the state of EBV infection. Although EBNA1 is thought to be a promising antigen for immunotherapy of all EBV-associated malignancies, it is less clear whether EBNA1-specific CD4+ T cells can act as direct effectors. Herein, we investigated the ability of CD4+ T-cell clones induced with overlapping peptides covering the C-terminal region of EBNA1, and identified minimal epitopes and their restricted major histocompatibility complex class II molecules. Of these, a novel epitope, EYHQEGGPD, was found to be presented by DRB1*0401, 0403 and 0406. Five CD4+ T-cell clones recognized endogenously processed and presented antigens on EBV-transformed lymphoblastoid cell lines (LCL) and one example proved capable of killing EBV-carrying natural killer (NK) and T-cell lines derived from patients with chronic active EBV infection (CAEBV). Identification of minimal epitopes facilitates design of peptide-based vaccines and our data suggest that EBNA1-specific CD4+ T cells may play roles as direct effectors for immunotherapy targeting EBV-carrying NK and T-cell malignancies. (*Cancer Sci* 2008; 99: 1633–1642)

The Epstein–Barr virus (EBV) is involved in development of many malignancies, including Burkitt's lymphoma (BL), Hodgkin's disease (HD) and the nasopharyngeal carcinoma, as well as post-transplant lymphoproliferative disorder.[1] It is also related to natural killer (NK) and T lymphomas and causes chronic active EBV infection (CAEBV).[1,2] Only EBV nuclear antigen (EBNA)1 is expressed in most BL, referred to as latency I. In addition to EBNA1, latent membrane protein (LMP)1 and/or 2 are expressed in HD, nasopharyngeal carcinomas, NK and T lymphomas, and CAEBV (latency II). All EBV latent antigens, EBNA1, 2, 3A, 3B, 3C and the leader protein, and LMP1 and 2 are expressed in post-transplant lymphoproliferative disorder (latency III). EBNA1 is expressed in common in all these diseases,[3] and may be present diffusely bound to mitotic chromosomes.[4] EBV has a *cis*-acting element, termed OriP, that enables the persistence of episomes in EBV-infected cells. EBNA1 also binds to OriP,[5] and is essential for EBV episome maintenance.[6] Thus, the existence of EBV DNA is tightly associated with EBNA1 expression in EBV-infected cells.

Evidence for the significance of EBV-specific T cells for control of EBV infection has been obtained from both *in vitro* and *in vivo* studies.[7,8] Human leukocyte antigen (HLA) class I-restricted CD8+ cytotoxic T lymphocytes (CTL) recognize latent and lytic EBV antigens,[8] and latent EBV antigen-specific CTL kill not only lymphoblastoid cell lines (LCL) expressing the full spectrum of latent viral proteins but also tumor cells with limited viral proteins.[9–11] EBV-specific CTL responses have been extensively studied, and CTL are thought to be the main effectors. EBNA1-specific CTL were long believed to be immunologically silent because EBNA1 contains an internal G-A repeat (GAr) domain which has an immune evasion function endowing resistance to proteasomal degradation in the antigen presentation pathway.[12,13] However, it has been reported that having GAr EBNA1 does not completely evade major histocompatibility complex (MHC) class I presentation.[10,14–16] There are thus some EBNA1 antigen epitopes, though the importance of EBNA1-specific CTL for EBV-positive tumors remains unclear.

Accumulating current evidence indicates that CD4+ T cells, as well as CTL, are required for effective antitumor immunity,[17–19] for example, playing an essential role in generation of CD8+ T memory cells.[20–22] In addition, there are reports of cytotoxic action of CD4+ T effector cells *in vitro*[23] and *in vivo*.[23,24] This has drawn attention to the possibility that EBV-specific CD4+ T cells are able to recognize EBV-infected cells. There is increasing interest in CD4+ T-cell responses to EBV as direct effectors. HLA class II-restricted CD4+ T cells specific for EBV latent and lytic antigens have been explored,[25–27] with the focus on EBV-infected B cells, mainly LCL, in which the HLA class II pathway of antigen presentation is active. Because immunoglobulin (Ig) isotype switching requires T-cell help, the presence of IgG antibodies to antigens implies that the latter are also targets of CD4+ T-cell responses.[28,29] Actually, healthy virus carriers are consistently positive for anti-EBNA1 IgG antibodies,[1] implying the existence of EBNA1-specific CD4+ T cells *in vivo*, because CD4+ T cells indeed recognize EBNA1 in healthy EBV carriers.[30,31] EBNA1 has been considered a promising antigen for T-helper (Th) cells. Moreover, it is clear that CD4+ T cells specific for EBNA1 can act as direct effectors for lysing BL cells and HD cells *in vitro*.[32] Furthermore, in a mouse model of BL, EBNA1-specific CD4+ T cells could suppress BL tumor growth *in vivo*.[33]

We report here the identification of five EBNA1-specific CD4+ T-cell clones recognizing LCL and their minimal epitopes. One HLA-DR4-restricted example is novel and the other four appear to be parts of longer peptides,[25,31] some of which are presented by other HLA class II molecules than those determined in this report. Of particular interest is a CD4+ T-cell clone killing EBV-infected T cells positive for DR51 and EBV-infected NK cells transduced with DRB5*0101. Because these EBV-infected NK and T cells express DR, DP and DQ, they could be potential targets of CD4+ T cells. These results imply that EBNA1-specific CD4+ T cells may also act as direct effectors *in vivo*.

[7]To whom correspondence should be addressed. E-mail: kkuzushi@aichi-cc.jp

doi: 10.1111/j.1349-7006.2008.00852.x

Table 1. Human leukocyte antigen (HLA) class II genotype of the donors and cell lines

Donors or cell lines	DRβ1	Other DR alleles	DPβ1	DQβ1
Donor X	*0401, *1501	DRβ4*0102, DRβ5*0101	*0201, *1401	*0301, *0602
Donor W	*0803, *1401	DRβ3*0202, NA	*0202, *0501	*0601, *0503
A1 LCL	*0101, *1401	DRβ3*0202, NA	*0402, *0501	*0501, *0502
A2 LCL	*0901, *0901	DRβ4*0103, DRβ4*0103	*0201, *0901	*0303, *0303
SNK10	*0901, *0901	DRβ4*0103, DRβ4*0103	*0201, *0402	*0303, *0303
SNT15	*0101, *0406	DRβ4*0103, NA	*0201, *0402	*0302, *0501
SNT16	*1201, *1502	DRβ3*0101, DRβ5*0102	*0501, *0901	*0303, *0601

NA, not assayed. LCL, lymphoblastoid cell lines.

Materials and Methods

Donors and cell lines. The study design and purpose, which had been approved by the institutional review board of Aichi Cancer Center, were fully explained and informed consent was obtained from all blood donors. HLA typing was carried out at the HLA Laboratory (Kyoto, Japan). The HLA class II genotype from donors X and W, and cell lines are shown in Table 1.

Epstein–Barr virus-transformed B-LCL were established as described previously,[34] and cultured in RPMI-1640 medium supplemented with 10% fetal calf serum, 2 mM L-glutamine, 50 U/mL penicillin, 50 μg/mL streptomycin and 50 μg/mL kanamycin.

An EBV-carrying NK cell line, SNK10, and an EBV-carrying γδ T-cell line, SNT15, and an EBV-carrying αβ T-cell line, SNT16, were kindly provided by Dr Shimizu (Tokyo Medical and Dental University, Tokyo, Japan). All three were derived from different CAEBV patients and cultured as previously described,[35,36] along with HEK-293 T cells. CD40-activated B (CD40-B) cells were generated as detailed earlier,[37,38] using NIH/3T3-human CD40 ligand cells, kindly provided by Dr Freeman (Dana-Farber Cancer Institute, Boston, MA, USA).

Phoenix-GALV cells kindly provided by Dr Kiem (Fred Hutchinson Cancer Research Center, Seattle, WA, USA) and Dr Nolan (Stanford University School of Medicine, Stanford, CA, USA) were cultured as previously described.[39] Retroviral transduction of HLA genes was performed as reported earlier.[37]

Plasmid construction. HLA-DRA cDNA were amplified by polymerase chain reaction (PCR) using a sense primer, 5′-ggatccgccaccATGGCCATAAGTGGAGTCCCTG-3′, and an antisense primer, 5′-gcggccgcTTACAGAGGCCCCCTGCGTTC-3′. The following primer pairs were used for PCR amplification of HLA-DRB1*0401 cDNA, HLA-DRB1*1501 cDNA, HLA-DRB4*0102 cDNA and HLA-DRB5*0101 cDNA: DRB1*0401 sense primer, 5′-ggatccgccaccATGGTGTGTCTGAAGTTCC-3′; DRB1*0401 antisense primer, 5′-gcggccgcTCAGCTCAGGAATCCTGTTG-3′. DRB1*0403, 0405 and 0406 cDNA were amplified by PCR with the DRB1*0401 sense primer and an antisense primer: DRB1*1501 sense primer, 5′-ggatccgccaccATGGTGTGTCTGAAGCTCC-3′ (fwd-1); DRB1*1501 antisense primer, 5′-gcggccgcTCAGCTCAGGAATCCTGTTG-3′; DRB4*0102 sense primer, fwd-1; DRB4*0102 antisense primer, 5′-gcggccgcTCAGCTCAAGAGTCCTGTTG-3′; DRB5*0101 sense primer, fwd-1; and DRB5*0101 antisense primer, 5′-gcggccgcTCAGCTCACGAGTCCTGTTG-3′. The resultant individual DNA fragments were cloned into pcDNA 3.1(+) using its *Bam*HI and *Not*I sites.

Full-length EBNA1 cDNA was cloned into pcDNA 3.1(+) (pcDNA/EBNA1).[16] EBNA1 without GAr (referred to as ΔGA-EBNA1) was constructed from pcDNA/EBNA1, as described previously.[40] The resulting construct was deleted from the GAr domain (EBNA1 codons 92–323).

Synthetic peptides. C-terminal EBNA1 polypeptides covering its 402–624 amino acids (a.a.) were deduced from the prototype B95-8 (National Center for Biotechnology Information accession no. V01555) DNA sequence. A total of thirty 20-mer peptides overlapping by 13 a.a. were designed, and purchased from Bio-Synthesis (Lewisville, TX, USA). A six-subpool was constructed from four to five peptides, excluding peptides including HLA class I-restricted epitopes. For example, HLA-B35-seropositive donors might be expected to respond to HPVGEADYFEY, and epitope-specific $CD8^+$ T cells might be expanded. Other known epitopes were excluded as well. To identify the core epitope sequence, 13- and 11-mer peptides were further designed and purchased from Bio-Synthesis. The one-letter a.a. code is used throughout the article.

Generation of $CD4^+$ T-cell lines and clones. Peripheral blood mononuclear cells (PBMC) from two donors were stimulated with individual peptide pools of 500 nM of each peptide in 2 mL RPMI-1640 medium supplemented with 10% human serum, 2 mM L-glutamine, 50 U/mL penicillin, 50 μg/mL streptomycin and 50 μg/mL kanamycin at 5% CO_2 in a humidified incubator. On days 8 and 15, T cells were restimulated with peptide-pulsed γ-irradiated (33 Gy) autologous PBMC. One day after each restimulation, interleukin (IL)-2, kindly provided by Ms Sawada (Shionogi, Osaka, Japan), was added to a final concentration of 10 U/mL. After four rounds of stimulation, $CD4^+$ T cells were isolated with CD4 Microbeads (Miltenyi Biotec, Tokyo, Japan).

To establish T-cell clones, limiting dilution of isolated $CD4^+$ T cells was performed as previously described,[41] with slight modifications. Where necessary, EBNA1 peptide-reactive $CD4^+$ T cells were enriched from restimulated $CD4^+$ T cells using an γ-interferon (IFN-γ) Secretion Assay (Miltenyi Biotec), according to the manufacturer's instructions. Then, the purified $CD4^+$ T cells were seeded at 1 cell/well in round-bottomed 96-well plates in culture medium containing anti-CD3 monoclonal antibodies (mAb) (30 ng/mL), IL-2 (200 U/mL), γ-irradiated (33 Gy) 1×10^5 PBMC and γ-irradiated (55 Gy) 2×10^4 LCL. After 14–16 days of culture, the specificity of growing cells was examined with enzyme-linked immunosorbent spot (ELISPOT) assays of EBNA1 peptide-pulsed CD40 B cells and autologous LCL. Positive wells were transferred into flasks and expanded with anti-CD3 mAb, IL-2 (30 U/mL) and γ-irradiated feeders.

ELISPOT assays. ELISPOT assays were performed as previously described,[37,41] with minor modifications. Briefly, $CD4^+$ T cells were co-cultured with various stimulators for 20 h in AIM-V medium (Invitrogen, Carlsbad, CA, USA) in wells of Multiscreen-HA plates (MAHA S4510; Millipore, Billerica, MA, USA) coated with antihuman IFN-γ mAb (M700A; Pierce Biotechnology, Philadelphia, PA, USA). As stimulators, LCL (1×10^5 cells/well), HEK-293 T cells (5×10^4 cells/well) transfected with plasmids encoding HLA-DRA and DRB1 cDNA, and/or ΔGA-EBNA1 or EGFP,[37] cDNA with Lipofectamin 2000 (Invitrogen) 36 h earlier were seeded into each well. For peptide titration assays, serial concentrations of synthetic peptides were pulsed to HLA-DR-expressing HEK-293T (referred to as DR-293T) cells for 1 h at room temperature. In blocking assays, anti-HLA-DR mAb (L243; BD Bioscience, San Jose, CA, USA), anti-HLA-DQ mAb (TÜ169; BD Bioscience), and anti-HLA-DP mAb (BRA-FB6; MorphoSys,

doi: 10.1111/j.1349-7006.2008.00852.x

Kingston, NH, SUA) were added at the indicated concentrations, and incubated for 1 h prior to co-cultivation with T cells. After probing with polyclonal antirabbit IFN-γ antibody (P700; Pierce Biotechnology), and following exposure to horseradish peroxidase-labeled antirabbit IgG antibody and spot visualization, the plates were washed and dried. IFN-γ spots were enumerated using a dissecting microscope. In all experiments using $CD4^+$ T cell clones, results from ELISPOT assays are shown as the mean of two duplicate values.

CTL assays. Target cells were labeled with 1.85 MBq chromium (^{51}Cr) for 1.5 h at 37°C, washed and mixed with CTL at the indicated effector to target ratios in 96-well plates. After incubation for 14 h at 37°C, the radioactivity in the supernatants was counted in a γ-counter. The minimal release was less 30% of maximal release in all experiments. The percentage-specific ^{51}Cr release was calculated as follows: 100 × (experimental release – spontaneous release)/(maximum release – spontaneous release). All assays were done in triplicate wells. Standard deviations were calculated from each data.

Results

Induction of EBNA1-specific $CD4^+$ T cells. It has been reported that $CD4^+$ T-cell epitopes are concentrated within the C-terminal of the EBNA1 protein,[25,31,32] and we designed 30 peptides (20-mers overlapping by 13 residues) covering a.a. 402–624. To generate EBNA1-specific $CD4^+$ T cells, PBMC from two EBV-seropositive donors were stimulated with 6-peptide pools. After four rounds of stimulation, $CD4^+$ T cells were isolated using CD4 Microbeads and ELISPOT assays were performed to test the specificity of the $CD4^+$ T-cell lines. As shown in Fig. 1(a,b), X1, X3 and X4 $CD4^+$ T-cell lines and W4 and W5 $CD4^+$ T-cell lines specifically secreted IFN-γ in response to cognate peptide pool-pulsed autologous CD40-B cells, but not to irrelevant peptide pool-pulsed CD40-B cells.

To further assess IFN-γ secretion against each peptide, $CD4^+$ T-cell lines were tested against peptides belonging to each pool. As illustrated in Fig. 2(a), production of IFN-γ by the X1 $CD4^+$ T-cell line from donor X was raised by two peptides (residues 409–428 and 416–435). Interestingly, the X3 $CD4^+$ T-cell line recognized three peptides (residues 472–491, 479–498 and 486–505) (Fig. 2b). Fig. 2(c) shows that the X4 $CD4^+$ T-cell line responded to two peptides (residues 514–533 and 521–540). As shown in Fig. 2(d, e), the W4 $CD4^+$ T-cell line recognized one peptide (residues 514–533) and the W5 $CD4^+$ T-cell line recognized two (residues 563–582 and 570–589).

Identification of the EBNA1 epitope. We established five $CD4^+$ T-cell clones by limiting-dilution culture of $CD4^+$ T-cell lines. As expected from the specificity of the X3 $CD4^+$ T-cell line, the derived clones X3-11D1 and X3-3G2 responded to two distinct peptides. ELISPOT assays were performed to map the recognized epitope regions (Figs 3,4). Because clone X1-12B12 secreted IFN-γ in response to two overlapping peptides (residues 409–428 and 416–435, Fig. 2a), the epitope was speculated to be located around a.a. residues 416–428. We attempted to identify minimal epitopes despite the fact that they may not be as definitive as those recognized by $CD8^+$ T cells because MHC class II molecules can present peptides with various lengths.[42,43] To this end, 13- and 11-mer peptides spanning the overlapped regions were synthesized and tested in ELISPOT assays to explore the N- and C-terminal a.a. which are indispensable for recognition. As shown in Fig. 3(a), deletion of E at position 416 (referred to as E_{416}) from the 13-mer peptide abolished the IFN-γ production from clone X1-12B12. At the C-terminus, loss of G_{425} from the 11-mer peptide had the same effect. Accordingly we infer that the a.a. sequence, EYHQEGGPDG, is a putative minimal epitope for the clone recognition. Fig. 4(a) additionally demonstrates that a 13-mer peptide, (F)EYHQEGGPDG(EP), containing the minimal epitope

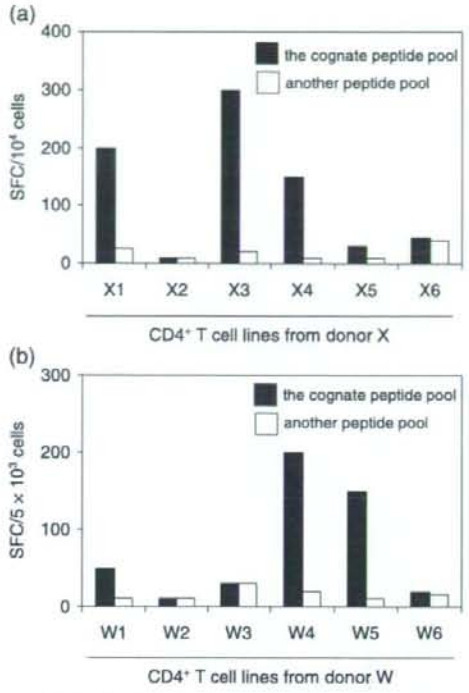

Fig. 1. Establishment of $CD4^+$ T-cell lines specific for Epstein–Barr virus nuclear antigen (EBNA)1 peptide pools. (a,b) Aliquots of peripheral blood mononuclear cells from donors X and W were stimulated *in vitro* with synthetic peptide pools four times. After CD4-positive selection, the responder cells were evaluated for their reactivity to the cognate peptide pools by enzyme-linked immunosorbent spot assays using autologous CD40-B cells as antigen-presenting cells. Another EBNA1 peptide pool that had not used in stimulation was tested for control. Data are numbers of spots per 10 000 $CD4^+$ T cells in (a) and 5000 $CD4^+$ T cells in (b). SFC, spot forming units.

sequence was better recognized than the 11-mer, (F)EYHQEGGPDG, and 13-mer, EYHQEGGPDG(EPD), peptides suggesting elongation of both N- and C-termini may augment the antigenicity.

As illustrated in Fig. 3(b), removal of P_{476} from 13- and 11-mer peptides completely abolished clone X3-11D1 recognition. The 13- and 11-mer peptides having R_{486} at the C-terminal stimulated the clone X3-11D1 to secrete IFN-γ. Thus, clone X3-11D1 responded to PKFENIAEGLR as the putative minimal epitope. Moreover, it recognized (SN)PKFENIAEGLR and (N)PKFENIAEGLR(A) more efficiently than the putative minimal epitope, PKFENIAEGLR (Fig. 4b).

As demonstrated in Fig. 3(c), deletion of L_{488} from the 13-mer peptide abolished the clone X3-3G2 recognition and IFN-γ secretion was also eliminated by deletion of R_{496} from the 13- and 11-mer peptides. This implies that LLARSHVER is the putative minimal epitope for the clone recognition. Furthermore, clone X3-3G2 could secrete IFN-γ in response to (RA)LLARSHVER(TT) and LLARSHVER(TTDE) as well as a 20-mer peptide (Fig. 4c).

As shown in Fig. 3(d), lack of R_{522} and L_{533} from 13-mer peptides abolished the clone X4-2C9 recognition. Accordingly, RGTALAIPQCRL is the putative minimal epitope required for IFN-γ secretion by clone X4-2C9, which did not respond to any 11-mer peptides. Moreover, clone X4-2C9 responded to 20-mer better than 13-mer peptides (Figs 3d, 4d).

As shown in Fig. 3(e), deletion of T_{568} from the 13-mer peptide abolished the IFN-γ production by clone W5-9D5, as did loss of